Electronic Journal of Mathematical Analysis and Applications
Vol. 11(2) July 2023, No. 12
ISSN: 2090-729X (online)
http://ejmaa.journals.ekb.eg/

*O*N SPATIO-TEMPORAL DYNAMICS OF COVID-19 EPIDEMIC $SE_1E_2I_1I_2RS$ MODEL INCORPORATING VIRUS MUTATIONS AND VACCINATIONS EFFECTS

A. A. ELSADANY[1,2], SARAH ALJUAIDI [1] AMR ELSONBATY[1,3], A. ALDURAYHIM[1]

ABSTRACT. This work is devoted to present temporal-only and spatio-temporal COVID-19 epidemic models when virus mutations and vaccination influences are considered. Firstly, the proposed non-diffusive COVID-19 model is introduced. The nonlinear incidence rate is employed to better model the strict measures forced by governmental authorities to control pandemic spread. The immunity acquired by vaccinations are assumed to be incomplete for realistic considerations. The existence, uniqueness and continuous dependence on initial conditions are studied for the solution. The study of stability along with bifurcation analysis are carried out to investigate the influences of variations in model's parameters. Moreover, the basic reproduction number is obtained for the proposed model. The stability regions for equilibrium points are depicted in space of parameters to explore their effects. Secondly, the diffusive version of the model is considered where possible occurrence of Turing instability is investigated. Finally, numerical simulations are employed to verify theoretical results of the work.

1. INTRODUCTION

Mathematical models are used to describe, better interpret and understand the various behaviors observed in nonlinear systems which arise in different disciplines of sciences such as engineering, biology, physics, astronomy, chemistry, economy, ...etc. The mathematical formulation of natural and man-made systems usually leads to a dynamical system whose independent variable is time. The goal of dynamical systems theories is to provide adequate tools to analyze and understand the nonlinear behaviors and the associated qualitative changes with parameters variations in mathematical models of the several deterministic processes found in life [1-9].
In general, dynamical systems can be classified into two main categories , namely, the iterated maps and the differential equations [1-4]. The proper mathematical formulation of dynamical model depends on the

2010 *Mathematics Subject Classification.* 37C10, 37G10, 37H20, 37N25.
Key words and phrases. COVID-19 virus, mutations, vaccination, epidemics, basic reproduction number, bifurcations..
Submitted Aug. 2023.

nature of explored phenomena and systems. Bifurcation analysis is employed to examine critical values of parameters at which the dynamical behavior of the nonlinear system undergoes qualitative changes. The bifurcation analysis of a dynamical system enables researchers to explore and predict possible stable/unstable dynamics and relate them to different regions in space of parameters. Therefore, the theories and methods of bifurcations along with numerical simulation techniques are inevitable tools for mathematicians, engineers, theoretical ecologists, etc. The applications in the field of dynamical systems involve physical sciences , engineering, neuroscience, mathematical biology, epidemiology,financial systems, biomedical engineering ,wave propagation , chemical kinetics, astronomy and even the more recent machine learning schemes [1-12]

The study of infectious diseases is one of the old and interesting areas in mathematical biology [13, 14]. Epidemic models simulate infectious diseases spread based on specific assumptions on parameters and state variables [15], and study how to eliminate and/or control disease spread.
Epidemic models usually classify human population into specific compartments according to their state and response to the infectious disease. In most conventional epidemic models, there are Susceptible (S), Infected (I), and Removed (R) individuals where the model in this case is denoted as SIR model [16, 17]. In other cases, the recovered individuals can loss their immunity and return back to S compartment. The epidemic model of this case is known as SIRS model. Mathematical models for epidemic forecasting can account for diversity in the early growth dynamics of epidemics and gain a sufficient understanding of the mechanisms at epidemics for rapid appreciation of potentially imperious situations then control them [18].

The Covid-19 pandemic, is a global pandemic induced by the Coronavirus (SARS-CoV-2) disease [19]. The first cases observed for this disease have been reported in December 2019 in Wuhan, Hubei, China [20]. Subsequently, it results in a worldwide spread and thus it has been announced as a pandemic on 11 March 2020 by world health organization. The first COVID-19 positive cases in Saudi Arabia came from Iran through Bahrain. They have been right away isolated and reported by the Ministry of Health as the first confirmed cases in the Kingdom of Saudi Arabia [21]. It is confirmed that the disease may be asymptomatic or may range from mild to very severe symptoms. According to the data gained in recent studies, the severity of the disease varies epidemiologically according to age, race and gender [22] and highly affects elderly people and those with comorbidities. Several outbreaks have occurred in health care settings [23]. The most observed symptoms for COVID-19 disease are cough, fever [24], vertigo, continued fatigue, and throb [24]. The highest peril of transmission may be caused by those having mild symptoms and not seeking medical counsel or those who are infectious through the incubation period [25] which lasts from 1 to 14 days [26].
In order to slow down the infections and control their spread, most governments have conducted many measures. These measures include schools and universities closure, adopting online-learning, social distancing, infected individuals isolation or quarantine, restricted travel, mall closure, curfew, mask wearing, exhort to avoid touching the nose, mouth and eyes,... etc [27, 28, 29].

The most recent statistics reveal that around $827,004$ confirmed cases of COVID-19 have been reported in Saudi Arabia with 9518 deaths cases. Several types of vaccines have been developed and used in the world in the last two years such as Pfizer, Moderna and AstraZeneca. For example, the number of vaccine doses administered in Saudi Arabia is $69,198,422$ for $26,983,197$ persons.

On other-hand, genetic changes or mutations of viruses are common phenomenon in epidemics. When a virus replicates, the copying of composing genes may subject to copying errors. These genetic mutations can accumulate within time and result in alterations in the proteins of virus surface or antigens. For example, the Alpha coronavirus causes severe lower respiratory tract infections in elderly and the children , the Beta coronavirus cause common cold [30] , and the Gamma has similar mutations to the Alpha and Beta strains [31]. The Delta coronavirus mutation has an advanced rate of spread and infection compared with other the

mutations [24]. Omicron is a highly infectious mutant strain of COVID-19 virus [32] where the reports from the African Medical Association displayed that omicron is seven times more infectious than the delta [24]. The World Health Organization designated omicron as of major concern [33].

Efficient mathematical models have been introduced to study other infectious diseases. In [34], a time-fractional order epidemic model of childhood diseases is solved by combining the classical homotopy perturbation method and Elzaki transform. A vaccination strategy, which offers temporary immunity, is studied in SIS epidemic model [35]. The reproduction number was found and its role of stability for equilibrium points were analyzed. Moreover, the relation between the efficiency of the vaccination and the reproduction number was investigated. The propagation of infection with a saturated incidence rate is considered in a discrete-time SIS model [36]. In [37], the bifurcation theory and direct numerical continuation are applied on a discrete Hindmarsh-Rose model, that describes neuronal behavior, to locate two-parameter bifurcation points. The fractional mathematical model of spread of vector-bone diseases was analysed in [38]. The authors of [39] studied discrete SIS model by assuming that the disease will not cause death where the vaccination program is considered.

The motivations of this study are summarized as follows:
(1) The reports of WHO and other health organizations indicate that around one third of COVID-19 confirmed cases do not develop any noticeable symptoms although they can infect others. Thus, it is essential to consider this point in the proposed COVID-19 model.
(2) Although there is a number of vaccines which have been approved and distributed in many countries, the ongoing COVID-19 virus mutations and genetic variants of concern may reduce the effectiveness of vaccines against them. Thus, it is essential to consider this issue in any realistic COVID-19 model.
(3) It is also observed that the COVID-19 pandemic waves can overwhelm emergency and medical services in areas of infections and can even sweep the most advanced countries in short time. Thus, the aggressive and strict control measures are inevitable to reduce the contact rate among infected and susceptible individuals. This implies that any reliable model should involve nonlinear incidence rate terms which accurately realize the influences of governmental actions on infection rates.
(4) The unrestricted movements of people between infected and non-infected regions can lead to a massive increase in number of infections. In China, for example, the reduction of quarantine procedures for travelers and closure policies for residents render the number of daily confirmed cases of COVID-19 around 29000 cases on December 23, 2022, compared with 121 confirmed cases on December 23, 2021. Hence, the individuals' movements and spatial influences should be considered to conduct more realistic modeling of COVID-19 pandemic.
The present work presents a more realistic model for COVID-19 pandemic. The proposed model simultaneously considers the following real-world scenarios:
(1) The model comprises the influences of infected individuals who do not develop any noticeable symptoms but can infect others.These state variables are separated from infectious state variables for individuals having noticeable symptoms.
(2) The influences of virus mutations and genetic variants of COVID-19 virus are also covered in the present model. The cases where efficacy of a vaccine is reduced by mutant strains of COVID-19 are also encompassed in the suggested model.
(3) The nonlinear incidence rate is adopted instead of the simple linear incidence rate. This accurately simulates the influences of governments control measures on infection rates of COVID-19 virus.
(4) The spatio-temporal influences are included in the proposed reaction-diffusion version of the model.
Therefore, the aim of the work is to present a more realistic COVID-19 model incorporating the influences of vaccinations programs, which have been undertaken worldwide and the recent mutations of coronavirus. The

nonlinear incidence rate of infection is adopted to involve the inhibition (psychological) effects. Moreover, the random motion of individuals of different compartments are included by considering reaction-diffusion version of the model. This paper is organized as follows: The $SE_1E_2I_1I_2RS$ mathematical model is presented in Section 2 followed by study of existence, uniqueness, and continuous dependence on initial conditions. Analysis of stability and bifurcations is carried out in Section 3 and the basic reproduction number is attained In Section 4. In Section 5, the diffusive COVID-19 model is introduced where Turing instability analysis is conducted. Numerical simulations are employed in Section 6 to verify theoretical results. Final discussion and conclusion are presented in Section 7.

2. The proposed non-diffusive model

In this section, the proposed $SE_1E_2I_1I_2RS$ COVID-19 epidemic model, which takes into account the mutant COVID-19 virus and vaccination programs, see Fig.1, is introduced in the following form

$$\begin{aligned}
\dot{S}(t) &= \mu - \beta_0 S E_1 - \beta_1 S E_2 - \frac{\beta_0 S I_1}{1+\alpha I_1^2} - \frac{\beta_1 S I_2}{1+\alpha I_2^2} + \delta R - (\upsilon + d)S,\\
\dot{E}_1(t) &= \beta_0 S E_1 - (\sigma_1 + \Omega_1 + c_1 + d)E_1,\\
\dot{E}_2(t) &= \beta_1 S E_2 - (\sigma_2 + \Omega_2 + c_2 + d)E_2,\\
\dot{I}_1(t) &= \frac{\beta_0 S I_1}{1+\alpha I_1^2} + \sigma_1 E_1 - (\gamma_1 + c_1 + d)I_1,\\
\dot{I}_2(t) &= \frac{\beta_1 S I_2}{1+\alpha I_2^2} + \sigma_2 E_2 - (\gamma_2 + c_2 + d)I_2,\\
\dot{R}(t) &= \Omega_1 E_1 + \Omega_2 E_2 + \gamma_1 I_1 + \gamma_2 I_2 + \upsilon S - (\delta + d)R,
\end{aligned} \tag{1}$$

where the state variables $[S(t), E_1(t), E_2(t), I_1(t), I_2(t), R(t)]$ and parameters of the model are describe in Table 1. For the primal COVID-19 virus, the infection rate is β_0, γ_1 denotes the rate of conversion from the infected state to the recover state, Ω_1 refers to the rate of progression from the exposed state to the recovered state. Also, σ_1 is the rate of conversion from the exposed state to the Infected state and the disease-related death rate is denoted by c_1. The associated rates for the mutant virus are β_1, γ_2, Ω_2, σ_2 and c_2. The parameter μ represents the birth rate whereas the disease-unrelated death rate is implemented by d. The parameter υ represents the vaccination rate of individuals whose state is transformed from susceptible to recovered state. However, for more realistic consideration, it is assumed that the immunity of vaccinated people can be lost by a rate of δ in the way that they return back to susceptible state. When the number of COVID-19 infections critically increases to high levels, the nonlinear incidence rates $\frac{\beta_i}{1+\alpha I_1^2}, i = 0, 1$ better reflect the strict measures forced by governmental authorities to control pandemic spread. The parameter α quantifies the strength of governmental actions and represents the inhibition effects on epidemic spread.

2.1. Existence and uniqueness.

The proposed model in (1) is written in the form

$$\dot{X}(t) = \Phi(X(t)),$$

$$t \in (0, T],$$

where $X(t) = [\ S \quad E_1 \quad E_2 \quad I_1 \quad I_2 \quad R\ ]^T$ and the initial condition is $X(0) = X_0$.

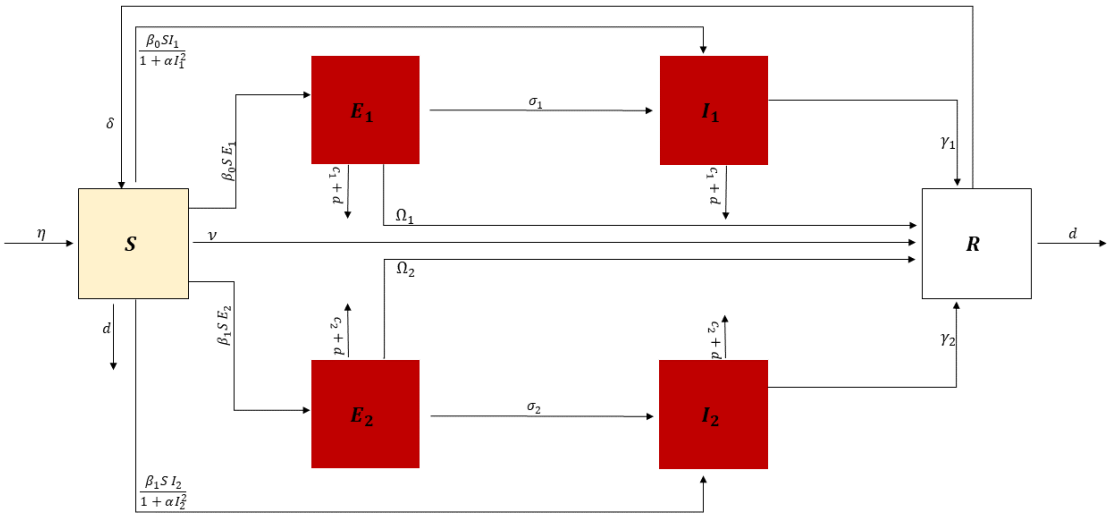

FIGURE 1. Flow diagram for the proposed $SE_1E_2I_1I_2RS$ COVID-19 epidemic model.

The solution of the above initial value problem can be expressed as

$$X(t) = X_0 + \int_0^t \Phi(X(\tau))d\tau. \tag{2}$$

The existence of this solution is investigated in the region $\Sigma \times J$ where

$$\Sigma = \{X(t) : max\,[|\xi|] < \Lambda\},$$

$$J = (0, T],$$

where ξ denotes state variables of the model. From the equivalence between integral equation (2) and the model system (1), and by referring to the right hand side of (2) as $\Psi(X)$, we get

$$\Psi(X_1) - \Psi(X_2) = \int_0^t (\Phi(X_1(\tau)) - \Phi(X_2(\tau)))d\tau.$$

The modulus is taken for both sides to obtain

$$\left|\Psi(X_1) - \Psi(X_2)\right| \leq \int_0^t \left|(\Phi(X_1(\tau)) - \Phi(X_2(\tau)))\right| d\tau,$$

which can be expressed as

TABLE 1. Definition of variables/parameters of the model.

Variable /Parameter	Definition
S(t)	Number of susceptible population
$E_1(t)$	Number of exposed to non-mutant virus population
$E_2(t)$	Number of exposed to mutant virus population
$I_1(t)$	Number of infected to non-mutant virus population
$I_2(t)$	Number of infected to mutant virus population
$R(t)$	Number of recovered / removed population
μ	The rate of birth
d	disease unrelated death rate
β_0	Non-mutant COVID-19 virus infection rate
β_1	Mutant COVID-19 virus infection rate
c_1	Non-mutant disease-related death rate
c_2	Mutant virus disease-related death rate
σ_1	Transformation rate from the exposed to non-mutant virus state to the infected state
σ_2	Transformation rate from the exposed to mutant virus state to the infected state
Ω_1	Transformation rate from the exposed to non-mutant virus state to the recover state
Ω_2	Transformation rate from the exposed to mutant virus state to the recover state
γ_1	Transformation rate from the infected by non-mutant virus state to the recover state
γ_2	Transformation rate from the infected by mutant virus state to the recover state
υ	The rate of people that have been vaccinated
δ	The loss of acquired immunity rate
α	Governmental action strength (inhibition effect)

$$\begin{cases} \left|S_1(t)-S_2(t)\right| \le \int_0^t \left|(\Phi_1(X_1(\tau))-\Phi_1(X_2(\tau)))\right| d\tau \\ \left|E_{11}(t)-E_{12}(t)\right| \le \int_0^t \left|(\Phi_2(X_1(\tau))-\Phi_2(X_2(\tau)))\right| d\tau \\ \left|E_{21}(t)-E_{22}(t)\right| \le \int_0^t \left|(\Phi_3(X_1(\tau))-\Phi_3(X_2(\tau)))\right| d\tau \\ \left|I_{11}(t)-I_{12}(t)\right| \le \int_0^t \left|(\Phi_4(X_1(\tau))-\Phi_4(X_2(\tau)))\right| d\tau \\ \left|I_{21}(t)-I_{22}(t)\right| \le \int_0^t \left|(\Phi_5(X_1(\tau))-\Phi_5(X_2(\tau)))\right| d\tau \\ \left|R_1(t)-R_2(t)\right| \le \int_0^t \left|(\Phi_6(X_1(\tau))-\Phi_6(X_2(\tau)))\right| d\tau \end{cases}$$

where $X_1(\tau)=[S_1,E_{11},E_{21},I_{11},I_{21},R_1]^T$ and $X_2(\tau)=[S_2,E_{12},E_{22},I_{12},I_{22},R_2]^T$.

Employing the two facts that

$$\begin{aligned} &\left|\beta_0 S_1 E_{11}-\beta_0 S_2 E_{12}\right| = \left|\beta_0 S_1 E_{11}-\beta_0 S_1 E_{12}+\beta_0 S_1 E_{12}-\beta_0 S_2 E_{12}\right| \\ &\le \beta_0 \Lambda \left|E_{11}-E_{12}\right| + \beta_0 \Lambda \left|S_1-S_2\right|, \quad 0<\frac{1}{1+\alpha I_i^2}\le 1, i=1,2 \end{aligned}$$

then the following inequality is attained

$$\left\|\Psi(X_1)-\Psi(X_2)\right\| \le \kappa \left\|X_1-X_2\right\|,$$

$$\begin{aligned} \kappa =& T max\{2\upsilon+d+4(\beta_0+\beta_1)\Lambda, 2\sigma_1+2\Omega_1+c_1+d+2\beta_0\Lambda, 2\sigma_2+2\Omega_2+c_2+d+2\beta_1\Lambda, \\ & 2\gamma_1+c_1+d+2\beta_0\Lambda, 2\gamma_2+c_2+d+2\beta_1\Lambda, 2\delta+d\} \end{aligned}$$

Note the supremum norm is utilized for the class of C^1 differentiable continuous functions on J.

Now we can formulate the next theorem about the sufficient condition for existence and uniqueness of the model (1).

Theorem 1 Assume that $\kappa = Tmax\{2\upsilon + d + 4(\beta_0 + \beta_1)\Lambda, 2\sigma_1 + 2\Omega_1 + c_1 + d + 2\beta_0\Lambda, 2\sigma_2 + 2\Omega_2 + c_2 + d + 2\beta_1\Lambda, 2\gamma_1 + c_1 + d + 2\beta_0\Lambda, 2\gamma_2 + c_2 + d + 2\beta_1\Lambda, 2\delta + d\} < 1$, then the solution of system (1) exists and it is unique on $\Sigma \times J$.

Proof. For $\kappa < 1$, the mapping $X = \Psi(X)$ is a contraction mapping and consequently the theorem follows directly from the fixed point theorem. ■

2.2. **Continuous dependence of initial conditions. Theorem 3** Suppose that the condition in Theorem 1 is satisfied, then the solution of system (1) exhibit continuous dependence on intial conditions that is for every $\epsilon > 0$ there exists $\rho > 0$ such that for two initial conditions X_{01}, X_{02} satsfying $\left|X_{01} - X_{02}\right| < \rho$, the solution trajectories achieve $\left|X_1(t) - X_2(t)\right| < \epsilon$.

Proof. The two solutions of the system (1) which start from the two close initial conditions $X_{01}$and $X_{02}$with

$$0 < \left|X_{01} - X_{02}\right| < \rho,$$

can be expressed as

$$X_1(t) = X_{01} + \int_0^t \Phi(X_1(\tau))d\tau,$$

$$X_2(t) = X_{02} + \int_0^t \Phi(X_1(\tau))d\tau.$$

Therefore, we get

$$\left\|X_1 - X_2\right\| \leq \left\|X_{01} - X_{02}\right\| + \kappa \left\|X_1 - X_2\right\|,$$

$$(1 - \kappa)\left\|X_1 - X_2\right\| \leq \left\|X_{01} - X_{02}\right\|,$$

where $0 < \kappa < 1$ as indicated above.

Put $\epsilon = \frac{\rho}{1-\kappa}$,then it is follows that

$$0 < \left\|X_1 - X_2\right\| < \epsilon,$$

whenever

$$0 < \left|X_{01} - X_{02}\right| < \rho.$$

■

3. Stability and bifurcation analysis

3.1. **Stability analysis.** The proposed model (1) has the following disease-free equilibrium point which corresponding to the disappearing of $E_1, E_2, I_1$and I_2

$$\Lambda = (\frac{(d+\delta)\mu}{d(d+\upsilon+\delta)}, 0, 0, 0, 0, \frac{\upsilon\mu}{d(d+\upsilon+\delta)})$$

Define the functions f_1, f_2, f_3, f_4, f_5 and f_6 as follows:

$$\begin{aligned}
f_1 &= \mu - \beta_0 S E_1 - \beta_1 S E_2 - \frac{\beta_0 S I_1}{1+\alpha I_1^2} - \frac{\beta_1 S I_2}{1+\alpha I_2^2} + \delta R - (\upsilon + d)S,\\
f_2 &= \beta_0 S E_1 - (\sigma_1 + \Omega_1 + c_1 + d)E_1,\\
f_3 &= \beta_1 S E_2 - (\sigma_2 + \Omega_2 + c_2 + d)E_2,\\
f_4 &= \frac{\beta_0 S I_1}{1+\alpha I_1^2} + \sigma_1 E_1 - (\gamma_1 + c_1 + d)I_1,\\
f_5 &= \frac{\beta_1 S I_2}{1+\alpha I_2^2} + \sigma_2 E_2 - (\gamma_2 + c_2 + d)I_2,\\
f_6 &= \Omega_1 E_1 + \Omega_2 E_2 + \gamma_1 I_1 + \gamma_2 I_2 + \upsilon S - (\delta + d)R.
\end{aligned} \tag{3}$$

Then define the following Jacobian matrix J in the form:

$$J = \begin{bmatrix}
f_{1S} & f_{1E_1} & f_{1E_2} & f_{1I_1} & f_{1I_2} & f_{1R}\\
f_{2S} & f_{2E_1} & f_{2E_2} & f_{2I_1} & f_{2I_2} & f_{2R}\\
f_{3S} & f_{3E_1} & f_{3E_2} & f_{3I_1} & f_{3I_2} & f_{3R}\\
f_{4S} & f_{4E_1} & f_{4E_2} & f_{4I_1} & f_{4I_2} & f_{4R}\\
f_{5S} & f_{5E_1} & f_{5E_2} & f_{5I_1} & f_{5I_2} & f_{5R}\\
f_{6S} & f_{6E_1} & f_{6E_2} & f_{6I_1} & f_{6I_2} & f_{6R}
\end{bmatrix},$$

where

$$f_{1S} = -d - \upsilon - E_1\beta_0 - E_2\beta_1 - \frac{I_1\beta_0}{1+I_1^4\alpha} - \frac{I_2\beta_1}{1+I_2^4\alpha}, f_{1E_1} = -S\beta_0, f_{1E_2} = -S\beta_1,$$

$$f_{1I_1} = \frac{2I_1^2 S\alpha\beta_0}{(1+I_1^2\alpha)^2}, f_{1I_2} = \frac{2I_2^2 S\alpha\beta_1}{(1+I_2^2\alpha)^2}, f_{1R} = \delta,$$

$$f_{2S} = E_1\beta_0, f_{2E_1} = -c_1 - d + S\beta_0 - \sigma_1 - \Omega_1, f_{2E_2} = 0, f_{2I_1} = 0, f_{2I_2} = 0, f_{2R} = 0,$$

$$f_{3S} = E_1\beta_1, f_{3E_1} = 0, f_{3E_2} = -c_2 - d + S\beta_1 - \sigma_2 - \Omega_2, f_{3I_1} = 0, f_{3I_2} = 0, f_{3R} = 0$$

$$f_{4S} = \frac{I_1\beta_0}{1+I_1^2\alpha}, f_{4E_1} = \sigma_1, f_{4E_2} = 0, f_{4I_1} = -c_1 - d - \frac{2I_1^2 S\alpha\beta_0}{(1+I_1^2\alpha)^2} + \frac{S\beta_0}{1+I_1^2\alpha} - \gamma_1, f_{4I_2} = 0, f_{4R} = 0$$

$$f_{5S} = \frac{I_2\beta_1}{1+I_2^2\alpha}, f_{5E_1} = 0, f_{5E_2} = \sigma_2, f_{5I_1} = 0, f_{5I_2} = -c_2 - d - \frac{2I_2^2 S\alpha\beta_1}{(1+I_2^2\alpha)^2} + \frac{S\beta_1}{1+I_2^2\alpha} - \gamma_2, f_{5R} = 0$$

$$f_{6S} = \upsilon, f_{6E_1} = \Omega_1, f_{6E_2} = \Omega_2, f_{6I_1} = \gamma_1, f_{6I_2} = \gamma_2, f_{6R} = -d - \delta$$

The Jacobian matrix for the model (1) evaluated at disease free state is given by:

$$J(\Lambda) = \begin{bmatrix}
-d-\upsilon & -\beta_0\Upsilon & -\beta_1\Upsilon & -\beta_0\Upsilon & -\beta_1\Upsilon & \delta\\
0 & -c_1 d + \beta_0\Upsilon - \sigma_1 - \Omega_1 & 0 & 0 & 0 & 0\\
0 & 0 & -c_2 d + \beta_1\Upsilon - \sigma_2 - \Omega_2 & 0 & 0 & 0\\
0 & \sigma_1 & 0 & -c_1 d + \beta_0\Upsilon - \gamma_1 & 0 & 0\\
0 & 0 & \sigma_2 & 0 & -c_2 d + \beta_1\Upsilon - \gamma_2 & 0\\
\upsilon & \Omega_1 & \Omega_2 & \gamma_1 & \gamma_2 & -d-\delta
\end{bmatrix},$$

where $\Upsilon = \frac{(d+\delta)\mu}{d(d+\upsilon+\delta)}$.
The eigenvalues λ of the matrix $J(\Lambda)$ are computed by solving the associated characteristic polynomial

$$\begin{aligned}
&(d+\lambda)(d+\upsilon+\delta+\lambda)(d(d+\upsilon+\delta)(c_1+d+\gamma_1+\lambda-\beta_0(d+\delta)\mu)(d(d+\upsilon+\delta)(c_2+d+\gamma_2+\lambda)-\beta_1(d+\delta)\mu)\\
&(d^3+c_1d(d+\upsilon+\delta)-d\beta_0\mu-\beta_0\delta\mu+d(\upsilon+\delta)(\lambda+\sigma_1+\Omega_1)+d^2(\upsilon+\delta+\lambda+\sigma_1+\Omega_1))\\
&(d^3+c_2d(d+\upsilon+\delta)-d\beta_1\mu-\beta_1\delta\mu+d(\upsilon+\delta\lambda+\sigma_2+\Omega_2+d^2(\upsilon+\delta+\lambda+\sigma_2+\Omega_2))=0.
\end{aligned} \tag{4}$$

The following eigenvalues can be then attained:

$$\begin{aligned}
\lambda_1 &= -d, \lambda_2 = -d-\upsilon-\delta, \lambda_3 = -\frac{d^3+c_1d(d+\upsilon+\delta)+d^2(\upsilon+\gamma_1+\delta)-\beta_0\delta\mu+d(\upsilon\gamma_1+\gamma_1\delta-\beta_0\mu)}{d(d+\upsilon+\delta)},\\
\lambda_4 &= -\frac{d^3+c_2d(d+\upsilon+\delta)+d^2(\upsilon+\gamma_2+\delta)-\beta_1\delta\mu+d(\upsilon\gamma_2+\gamma_2\delta-\beta_1\mu)}{d(d+\upsilon+\delta)},\\
\lambda_5 &= -\frac{d^3+c_1d(d+\upsilon+\delta)-d\beta_0\mu-d\beta_0\delta\mu+d(\upsilon+\delta)(\sigma_1\Omega_1)+d^2(\upsilon+\delta+\sigma_1+\Omega_1)}{d(d+\upsilon+\delta)},\\
\lambda_6 &= -\frac{d^3+c_2d(d+\upsilon+\delta)-d\beta_1\mu-d\beta_1\delta\mu+d(\upsilon+\delta)(\sigma_2\Omega_2)+d^2(\upsilon+\delta+\sigma_2+\Omega_2)}{d(d+\upsilon+\delta)}
\end{aligned}$$

If $\lambda_1, \lambda_2, \lambda_3, \lambda_4, \lambda_5$ andλ_6 are negative or have negative real parts then the disease free equilibrium point is locally asymptotic stable.
The endemic equilibrium point has very complicated form which render numerical investigation necessary to examine it. We use numerical simulation to find stability regions in space of parameters of the model in numerical simulations section.

3.2. **Bifurcation analysis.** Sotomayor's theorem is employed to explore the type of bifurcation which can be found in the proposed model.

Theorem 3.1. *Define*

$$\Upsilon = Df|_{(x=x_0,\xi=\xi_0)}$$

and suppose that Υ *has a single zero eigenvalue with* V, D *being the left and right eigenvectors, respectively, i.e* $\Upsilon V = 0$ *and* $W\Upsilon = 0$

Define also the following coefficients for the model

$$\begin{aligned}
A &= \frac{1}{V.W}W.\frac{\partial f}{\partial\xi}|_{(x=x_0,\xi=\xi_0)},\\
B &= \frac{1}{V.W}\sum_{i,j,k=1}^{n}W_iV_jV_k(.\frac{\partial^2 f_i}{\partial x_j\partial x_k})|_{(x=x_0,\xi=\xi_0)},\\
C &= \frac{2}{V.W}\sum_{i,j=1}^{n}W_iV_j(.\frac{\partial^2 f_i}{\partial x_j\partial\xi})|_{(x=x_0,\xi=\xi_0)}.
\end{aligned} \tag{5}$$

Then, if $A = 0$ *and* $B \neq 0 \neq C$, *the model undergoes transcritical bifurcation at the critical parameter* $\xi = \xi_0$

Consider the disease-free equilibrium point of the system (1). There is a critical value for parameter β_0 at $\beta_0 = \dfrac{d(c_1 + d + \gamma_1)(d + \upsilon + \delta)}{(d + \delta)\mu}$. Hence, we can find

$$V = \begin{bmatrix} -\dfrac{-c_1 d - d^2 - d\gamma_1 - c_1\delta - d\delta}{c_1\upsilon + d\upsilon + d\gamma_1} \\ 0 \\ 0 \\ -\dfrac{d^2 + d\upsilon + d\delta}{c_1\upsilon + d\upsilon + d\gamma_1} \\ 0 \\ 1 \end{bmatrix} \quad , \quad W = \begin{bmatrix} 0 & \dfrac{\sigma_1}{-\gamma_1 + \sigma_1 + \Omega_1} & 0 & 1 & 0 & 0 \end{bmatrix},$$

and then $V.W = -\dfrac{d^2 + d\upsilon + d\delta}{c_1\upsilon + d\upsilon - d\gamma_1}$.

The critical coefficients are obtained as follows

$A = 0$, $B = \dfrac{2d(c_1 + d + \gamma_1)(d + \upsilon + \delta)(c_1(d + \delta)) + d(d + \gamma_1 + \delta)}{(c_1\upsilon + d(\upsilon - \gamma_1)(d + \delta)\mu}$ and $C = \dfrac{2(d + \delta)\mu}{d(d + \upsilon + \delta)}$

and thus the type of bifurcation is transcritical bifurcation.

Now, consider the critical parameter value of β_1 which occurs at $\beta_1 = \dfrac{d(c_2 + d + \gamma_2)(d + \upsilon + \delta)}{(d + \delta)\mu}$. The associated eigenvectors are determined as

$$V = \begin{bmatrix} -\dfrac{-c_2 d - d^2 - d\gamma_2 - c_2\delta - d\delta}{c_2\upsilon + d\upsilon + d\gamma_2} \\ 0 \\ 0 \\ -\dfrac{d^2 + d\upsilon + d\delta}{c_2\upsilon + d\upsilon + d\gamma_2} \\ 0 \\ 1 \end{bmatrix} \quad , \quad W = \begin{bmatrix} 0 & \dfrac{\sigma_2}{-\gamma_2 + \sigma_2 + \Omega_2} & 0 & 1 & 0 & 0 \end{bmatrix},$$

with

$$V.W = -\frac{d^2 + d\upsilon + d\delta}{c_2\upsilon + d\upsilon - d\gamma_2}.$$

The corresponding critical coefficients are computed as

$A = 0$, $B = \dfrac{2d(c_2 + d + \gamma_2)(d + \upsilon + \delta)(c_2(d + \delta)) + d(d + \gamma_2 + \delta)}{(c_2\upsilon + d(\upsilon - \gamma_2)(d + \delta)\mu}$ and $C = \dfrac{2(d + \delta)\mu}{d(d + \upsilon + \delta)}$

and the bifurcation is a transcritical too.

Finally, the possible bifurcation at the critical value of γ_1 that is given by

$$\gamma_1 = -\frac{d^3 + d^2(\upsilon + \delta) + c_1 d(d + \upsilon + \delta) - d\beta_0\mu - \beta_0\delta\mu}{d(d + \upsilon + \delta)}$$

is also examined. It is found that

$$V = \begin{bmatrix} -\dfrac{c_1 d\delta - d^2\delta - c_1 \upsilon\delta - d\upsilon\delta - c_1\delta^2 - d\delta^2 - d\beta_0\mu - \beta_0\delta\mu}{c_1 d^2 + d^3 + 2c_1 d\upsilon + 2d^2\upsilon + c_1\upsilon^2 + d\upsilon^2 + c_1 d\delta + c_1\upsilon\delta + d\upsilon\delta - d\beta_0\mu - \beta_0\delta\mu} \\ 0 \\ 0 \\ -\dfrac{d^3 + 2d^2\upsilon + d\upsilon^2 + 2d^2\delta + 2d\upsilon\delta + d\delta^2}{c_1 d^2 + d^3 + c_1 d\upsilon + 2d^2\upsilon + c_1\upsilon^2 + d\upsilon^2 + c_1 d\delta + d^2\delta + c_1\upsilon\delta + d\upsilon\delta - d\beta_0\mu - \beta_0\delta\mu} \\ 0 \\ 1 \end{bmatrix},$$

$$W = \begin{bmatrix} 0 & \dfrac{d(d+\upsilon+\delta)\sigma_1}{d^3 + c_1 d(d+\upsilon+\delta) - d\beta_0\mu - \beta_0\delta\mu + d(\upsilon+\delta)(\sigma_1+\Omega_1) + d^2(\upsilon+\delta+\sigma_1+\Omega_1)} & 0 & 1 & 0 & 0 \end{bmatrix},$$

$$V.W = -\frac{d(d+\upsilon+\delta)^2}{d^3 + c_1(d+\upsilon)(d+\upsilon+\delta) + d^2(2\upsilon+\delta) - \beta_0\delta\mu + d(\upsilon^2 + \upsilon\delta - \beta_0\mu)}$$

Also, we get,

$$B = \frac{2\beta_0(d^2\delta + c_1\delta(d+\upsilon+\delta) + \beta_0\delta\mu + d(\upsilon\delta + \delta^2 + \beta_0\mu))}{d^3 + c_1(d+\upsilon)(d+\upsilon+\delta) + d^2(2\upsilon+\delta) - \beta_0\delta\mu + d(\upsilon^2 + \upsilon\delta - \beta_0\mu)}$$

and $C = -2$. Then, the bifurcation is a transcritical bifurcation.

Numerical experiments are employed to verify above results in numerical simulations section.

4. Basic reproduction number

In model (1), the state variables $S_1(t)$, $S_2(t)$ and $R(t)$ represent the disease free compartments. On other side, the state variables $E_1(t)$,$E_2(t)$,$I_1(t)$,and $I_2(t)$ represent the infected compartments. The basic reproduction number R_0 is defined as the expected number of infection cases which can be caused by a single infected individual when all individuals in the population are susceptible to infection. It is a crucil parameter in epidemic model and can be used to indicate the possible long-term behaviour of the epidemic system. For $R_0 > 1$, the presence infected individual can start spreading the infection in the population. The spread of the infection can be suppressed if $R_0 < 1$. From practical point of view, the large value of R_0 implies that it is harder to control the pandemic.

Several techniques are used to estimate the value of R_0, and in particular, the well-known next generation matrix scheme has been widely employed in epidemics, see [40, 41, 42] and references therein. The system (1) can be expressed as

$$\frac{dX}{dt} = Y_1(X) - Y_2(X),$$

where

$$Y_1(X) = \begin{pmatrix} 0 \\ \beta_0 S E_1 \\ \beta_1 S E_2 \\ \frac{\beta_0 S I_1}{1+\alpha I_1^2} \\ \frac{\beta_1 S I_2}{1+\alpha I_2^2} \\ 0 \end{pmatrix},$$

$$Y_2(X) = \begin{pmatrix} -\mu + \beta_0 S E_1 + \beta_1 S E_2 + \frac{\beta_0 S I_1}{1+\alpha I_1^2} + \frac{\beta_1 S I_2}{1+\alpha I_2^2} - \delta R + (\upsilon + d)S \\ (\sigma_1 + \Omega_1 + c_1 + d)E_1 \\ (\sigma_2 + \Omega_2 + c_2 + d)E_2 \\ -\sigma_1 E_1 + (\gamma_1 + c_1 + d)I_1 \\ -\sigma_2 E_2 + (\gamma_2 + c_2 + d)I_2 \\ -\Omega_1 E_1 - \Omega_2 E_2 - \gamma_1 I_1 - \gamma_2 I_2 - \upsilon S + (\delta + d)R \end{pmatrix}.$$

Now, considering the disease free equilibrium point, the transmissions matrix Π_1 and transitions matrix Π_2 are obtained as follows

$$\Pi_1 = \begin{pmatrix} \frac{\beta 0(d+\delta)\mu}{d(d+\upsilon+\delta)} & 0 & 0 & 0 \\ 0 & \frac{\beta 1(d+\delta)\mu}{d(d+\upsilon+\delta)} & 0 & 0 \\ 0 & 0 & \frac{\beta 0(d+\delta)\mu}{d(d+\upsilon+\delta)} & 0 \\ 0 & 0 & 0 & \frac{\beta 1(d+\delta)\mu}{d(d+\upsilon+\delta)} \end{pmatrix},$$

$$\Pi_2 = \begin{pmatrix} c_1 + d + \sigma_1 + \Omega_1 & 0 & 0 & 0 \\ 0 & c_1 + d + \sigma_2 + \Omega_2 & 0 & 0 \\ -\sigma_1 & 0 & c_2 + d + \gamma_1 & 0 \\ 0 & -\sigma_2 & 0 & c_2 + d + \gamma_2 \end{pmatrix}.$$

The inverse of $\Pi_2$is found as follows

$$\Pi_2^{-1} = \begin{pmatrix} \frac{1}{c_1+d+\sigma_1+\Omega_1} & 0 & 0 & 0 \\ 0 & \frac{1}{c_1+d+\sigma_2+\Omega_2} & 0 & 0 \\ \frac{\sigma_1}{(c_2+d+\gamma_1)(c_1+d+\sigma_1+\Omega_1)} & 0 & \frac{1}{c_2+d+\gamma_1} & 0 \\ 0 & \frac{\sigma_2}{(c_2+d+\gamma_2)(c_1+d+\sigma_2+\Omega_2)} & 0 & \frac{1}{c_2+d+\gamma_2} \end{pmatrix},$$

and consequently we can get $\Pi_1 \Pi_2^{-1}$ The estimated basic reproduction number is given by

$$R_0 = Max\{\frac{\beta_0(d+\delta)\mu}{d(d+\upsilon+\delta)(c_1+d+\sigma_1+\Omega_1)}, \frac{\beta_0(d+\delta)\mu}{d(c_2+d+\gamma_1)(d+\upsilon+\delta)},$$

$$\frac{\beta_1(d+\delta)\mu}{d(d+\upsilon+\delta)(c_1+d+\sigma_2+\Omega_2)}, \frac{\beta_1(d+\delta)\mu}{d(c_2+d+\gamma_2)(d+\upsilon+\delta)}\}.$$

5. The diffusive COVID-19 model

As the model (1) considers an evolution between humans, it is of interest to analyse the spatial spread of those populations. This can be done by adding diffusion terms that gives a reaction diffusion version of the model 1.

The diffusion of the populations will be studied in two spatial dimensions. That is we will add $\nabla^2 = \frac{\partial^2}{\partial x^2} + \frac{\partial^2}{\partial y^2}$. Moreover, the movements of individuals are assumed random within their environments. This

consideration is realized by using self-diffusion. So, the diffusive COVID-19 version of the proposed model can be written as:

$$\begin{aligned}
\frac{\partial S}{\partial t} &= \mu - \beta_0 S E_1 - \beta_1 S E_2 - \frac{\beta_0 S I_1}{1+\alpha I_1^2} - \frac{\beta_1 S I_2}{1+\alpha I_2^2} + \delta R - (\upsilon + d)S + D_1 \nabla^2 S,\\
\frac{\partial E_1}{\partial t} &= \beta_0 S E_1 - (\sigma_1 + \Omega_1 + c_1 + d)E_1 + D_2 \nabla^2 E_1,\\
\frac{\partial E_2}{\partial t} &= \beta_1 S E_2 - (\sigma_2 + \Omega_2 + c_2 + d)E_2 + D_3 \nabla^2 E_2,\\
\frac{\partial I_1}{\partial t} &= \frac{\beta_0 S I_1}{1+\alpha I_1^2} + \sigma_1 E_1 - (\gamma_1 + c_1 + d)I_1 + D_4 \nabla^2 I_1,\\
\frac{\partial I_2}{\partial t} &= \frac{\beta_1 S I_2}{1+\alpha I_2^2} + \sigma_2 E_2 - (\gamma_2 + c_2 + d)I_2 + D_5 \nabla^2 I_2,\\
\frac{\partial R}{\partial t} &= \Omega_1 E_1 + \Omega_2 E_2 + \gamma_1 I_1 + \gamma_2 I_2 + \upsilon S - (\delta + d)R + D_6 \nabla^2 R,
\end{aligned} \tag{6}$$

where diffusion coefficients $D_1 - D_6$ take positive values. We confine our study on the stability of equilibrium points to examine if the diffusion terms destabilize the equilibrium state. In this case, the system (6) presents what is so called Turing patterns.

5.1. **Turing instability analysis.** Suppose that the equilibrium point:

$$(S^*, E_1^*, E_2^*, I_1^*, I_2^*, R^*) = \left(\frac{\mu(d+\delta)}{d(d+\delta+\upsilon)}, 0, 0, 0, 0, \frac{\mu\upsilon}{d(d+\delta+\upsilon)} \right) \tag{7}$$

is stable for the temporal-only version of the model.

The linearisation of the model (6) can be obtained by small perturbation, namely, $\mathbf{S}, \mathbf{E_1}, \mathbf{E_2}, \mathbf{I_1}, \mathbf{I_2}$ and $\mathbf{R}$ such that $S = S^* + \mathbf{S}$, $E_1 = E_1^* + \mathbf{E_1}$, $E_2 = E_2^* + \mathbf{E_2}$, $I_1 = I_1^* + \mathbf{I_1}$, $I_2 = I_2^* + \mathbf{I_2}$ and $R = R^* + \mathbf{R}$. Thus, the linear form of the system (6) is given as

$$\begin{aligned}
\frac{\partial S}{\partial t} &= f_{1S}\mathbf{S} + f_{1E_1}\mathbf{E_1} + f_{1E_2}\mathbf{E_2} + f_{1I_1}\mathbf{I_1} + f_{1I_2}\mathbf{I_2} + f_{1R}\mathbf{R} + D_1\nabla^2\mathbf{S},\\
\frac{\partial E_1}{\partial t} &= f_{2S}\mathbf{S} + f_{2E_1}\mathbf{E_1} + f_{2E_2}\mathbf{E_2} + f_{2I_1}\mathbf{I_1} + f_{2I_2}\mathbf{I_2} + f_{2R}\mathbf{R} + D_2\nabla^2\mathbf{E_1},\\
\frac{\partial E_2}{\partial t} &= f_{3S}\mathbf{S} + f_{3E_1}\mathbf{E_1} + f_{3E_2}\mathbf{E_2} + f_{3I_1}\mathbf{I_1} + f_{3I_2}\mathbf{I_2} + f_{3R}\mathbf{R} + D_3\nabla^2\mathbf{E_2},\\
\frac{\partial I_1}{\partial t} &= f_{4S}\mathbf{S} + f_{4E_1}\mathbf{E_1} + f_{4E_2}\mathbf{E_2} + f_{4I_1}\mathbf{I_1} + f_{4I_2}\mathbf{I_2} + f_{4R}\mathbf{R} + D_4\nabla^2\mathbf{I_1},\\
\frac{\partial I_2}{\partial t} &= f_{5S}\mathbf{S} + f_{5E_1}\mathbf{E_1} + f_{5E_2}\mathbf{E_2} + f_{5I_1}\mathbf{I_1} + f_{5I_2}\mathbf{I_2} + f_{5R}\mathbf{R} + D_5\nabla^2\mathbf{I_2},\\
\frac{\partial R}{\partial t} &= f_{6S}\mathbf{S} + f_{6E_1}\mathbf{E_1} + f_{6E_2}\mathbf{E_2} + f_{6I_1}\mathbf{I_1} + f_{6I_2}\mathbf{I_2} + f_{6R}\mathbf{R} + D_6\nabla^2\mathbf{R},
\end{aligned} \tag{8}$$

Suppose that the linear system (8) has a solution in the following form

$$\begin{bmatrix} \mathbf{S} \\ \mathbf{E_1} \\ \mathbf{E_2} \\ \mathbf{I_1} \\ \mathbf{I_2} \\ \mathbf{R} \end{bmatrix} = \mathcal{A} \exp(\lambda t) \exp(ikr), \tag{9}$$

where $\mathcal{A} = \begin{bmatrix} A_1 & A_2 & A_3 & A_4 & A_5 & A_6 \end{bmatrix}$ is a vector with no zero component, λ is time growth rate, k is a wave vector and $r \equiv (x, y)$ denotes space vector.

Substituting (9) into (8) gives the following system for the equilibrium point (7):

$$\begin{aligned} &A_1 d^3 + \left((A_1 - A_6)\delta + A_1\left(D_1 k^2 + \lambda + 2v\right)\right) d^2 + \\ &\left(-A_6\delta^2 + \left(\left(D_1 k^2 + \lambda + v\right) A_1 - vA_6\right)\delta + v\left(D_1 k^2 + \lambda + v\right) A_1 + \mu\left(\left(A_2 + A_4\right) b_0 + b_1\left(A_3 + A_5\right)\right)\right) d \\ &+ \mu\left(\left(A_2 + A_4\right) b_0 + b_1\left(A_3 + A_5\right)\right)\delta = 0, \end{aligned} \tag{10}$$

$$\begin{aligned} &(D_2 d^2 k^2 + D_2 d\delta k^2 + D_2 dk^2 v + \Omega_1 d^2 + \Omega_1 d\delta + \Omega_1 dv - b_0\mu d - b_0\delta\mu + cd^2 + cd\delta + cdv + d^3 + d^2\delta \\ &+ \lambda d^2 + d^2\sigma_1 + d^2 v + \lambda\delta d + d\delta\sigma_1 + d\lambda v + d\sigma_1 v)A_2 = 0, \end{aligned} \tag{11}$$

$$\begin{aligned} &(D_3 d^2 k^2 + D_3 d\delta k^2 + D_3 dk^2 v + \Omega_2 d^2 + \Omega_2 d\delta + \Omega_2 dv - b_1\mu d - b_1\delta\mu + cd^2 + cd\delta + cdv + d^3 + d^2\delta \\ &+ \lambda d^2 + d^2\sigma_2 + d^2 v + \lambda\delta d + d\delta\sigma_2 + d\lambda v + d\sigma_2 v)A_3 = 0 \end{aligned} \tag{12}$$

$$\begin{aligned} &A_4 d^3 + ((D_4 k^2 + c + \delta + \gamma + \lambda + v)A_4 - \sigma_1 A_2)d^2 + (((D_4 k^2 + c + \gamma_1 + \lambda)\delta + (D_4 k^2 + c + \gamma_1 + \lambda)v - b_0\mu)A_4 \\ &- \sigma_1 A_2(\delta + v))d - A_4 b_0\delta\mu = 0 \end{aligned} \tag{13}$$

$$\begin{aligned} &d^3 A_5 + ((D_5 k^2 + c + \delta + \gamma_2 + \lambda + v)A_5 - \sigma_2 A_3)d^2 + (((D_5 k^2 + c + \gamma_2 + \lambda)\delta + (D_5 k^2 + c + \gamma_2 + \lambda)v - b_1\mu)A_5 \\ &- \sigma_2 A_3(\delta + v))d - b_1\mu\delta A_5 = 0 \end{aligned} \tag{14}$$

$$(D_6 k^2 + d + \delta + \lambda)A_6 - \gamma_2 A_5 - \Omega_1 A_2 - \Omega_2 A_3 - \gamma_1 A_4 - A_1 v = 0 \tag{15}$$

As we seek nonzero A_is, one could arrange the equations (10)-(15) in a matrix form such following:

$$\mathcal{M}\mathcal{A} = \mathbf{0}, \tag{16}$$

where $\mathcal{M}$ is a 6×6 matrix has the following form

$$\mathcal{M} = \begin{bmatrix} \blacksquare & \blacksquare & \blacksquare & \blacksquare & \blacksquare & \blacksquare \\ 0 & \blacksquare & 0 & 0 & 0 & 0 \\ 0 & 0 & \blacksquare & 0 & 0 & 0 \\ 0 & \blacksquare & 0 & \blacksquare & 0 & 0 \\ 0 & 0 & \blacksquare & 0 & \blacksquare & 0 \\ \blacksquare & \blacksquare & \blacksquare & \blacksquare & \blacksquare & \blacksquare \end{bmatrix}$$

The linear system (16) has a nontrivial solution (i.e. $A_1 \times A_2 \times \cdots \times A_6 \neq 0$) if $|\mathcal{M}| = 0$. The form of the factors of the determinant of $\mathcal{M}$ is expressed as follows:

$$|\mathcal{M}| = \psi_1(\lambda)\,\psi_2(\lambda)\,\cdots\,\psi_5(\lambda), \tag{17}$$

where

$$\begin{aligned}\psi_1(\lambda) =&(d^2 + d\delta + dv)\lambda + D_2d^2k^2 + D_2d\delta k^2 + D_2dk^2v + \Omega_1d^2 + \Omega_1d\delta + \Omega_1dv - b_0d\mu \\ &- b_0\mu\delta + cd^2 + cd\delta + cdv + d^3 + d^2\delta + d^2\sigma_1 + d^2v + d\delta\sigma_1 + d\sigma_1v,\end{aligned} \tag{18}$$

$$\begin{aligned}\psi_2(\lambda) =&(d^2 + d\delta + dv)\lambda + D_3d^2k^2 + D3d\delta k^2 + D_3dk^2v + \Omega_2d^2 + \Omega_2d\delta + \Omega_2dv - b_1d\mu - b_1\mu\delta \\ &+ cd^2 + cd\delta + cdv + d^3 + d^2\delta + d^2\sigma_2 + d^2v + d\delta\sigma_2 + d\sigma_2v,\end{aligned} \tag{19}$$

$$\begin{aligned}\psi_3(\lambda) =&(d^2 + d\delta + dv)\lambda + D_4d^2k^2 + D_4d\delta k^2 + D_4dk^2v - b_0d\mu - b_0\mu\delta + cd^2 + cd\delta + cdv + d^3 \\ &+ d^2\delta + d^2\gamma_1 + d^2v + d\delta\gamma_1 + d\gamma_1v,\end{aligned} \tag{20}$$

$$\begin{aligned}\psi_4(\lambda) =&(d^2 + d\delta + dv)\lambda + D_5d^2k^2 + D_5d\delta k^2 + D_5dk^2v - b_1d\mu - b_1\mu\delta + cd^2 + cd\delta + cdv + d^3 \\ &+ d^2\delta + d^2\gamma_2 + d^2v + d\delta\gamma_2 + d\gamma_2v,\end{aligned} \tag{21}$$

and

$$\begin{aligned}\psi_5(\lambda) =&(d^2 + d\delta + dv)\lambda^2 + (D_1d^2k^2 + D_1d\delta k^2 + D_1dk^2v + D_6d^2k^2 + D_6d\delta k^2 + D_6dk^2v + 2d^3 \\ &+ 3d^2\delta + 3d^2v + d\delta^2 + 2d\delta v + dv^2)\lambda + D_1D_6d^2k^4 + D_1D_6d\delta k^4 + D_1D_6dk^4v + D_1d^3k^2 \\ &+ 2D_1d^2\delta k^2 + D_1d^2k^2v + D_1d\delta^2k^2 + D_1d\delta k^2v + D_6d^3k^2 + D_6d^2\delta k^2 + 2D_6d^2k^2v \\ &+ D_6d\delta k^2v + D_6dk^2v^2 + d^4 + 2d^3\delta + 2d^3v + d^2\delta^2 + 2d^2\delta v + d^2v^2.\end{aligned} \tag{22}$$

Simplifying the equations (18)-(22) and after some calculations, we conclude that there is no positive real parts which can be attained for λ. This implies that the stable equilibrium points do not lose its stability as a result of adding the diffusion terms.

6. Numerical simulations

Numerical simulations are carried out to verify theoretical results that have been obtained in previous sections. Firstly, we set the parameters of model (1) to the specific values which achieve stability of disease free equilibrium point. In Figure 2, the three dimensional phase portraits of the state variables in system (1) exhibit the local stability of disease free state for the following values of parameters: $\mu = 0.3, d = 0.05, \delta = 0.7, \gamma_1 = 0.4, \gamma_2 = 0.5, c_1 = 0.008, c_2 = 0.012, \sigma_1 = 0.7, \sigma_2 = 0.75, \Omega_1 = 0.8, \Omega_2 = 0.85, \upsilon = 0.75, \alpha = 1, \beta_0 = 0.15, \beta_1 = 0.1$. The basic reproduction number for this case is found to be less than one, which indicates that the infectious disease can be controlled.

Secondly, we further proceed to examine the influences of the parameters on stability of disease-free steady state to help control the epidemic spread via tuning the key parameters to appropriate values. The stability regions is blue-colored in different spaces of parameters in Figure (3) for different scenarios. In first scenario, we take $\mu = 0.3, d = 0.05, \beta_1 = 0.15, \delta = 0.7, \gamma_1 = 0.4, c_1 = 0.008, c_2 = 0.012, \gamma_2 = 0.5, \sigma_1 = 0.7, \sigma_2 = 0.75, \Omega_1 = 0.8, \Omega_2 = 0.85, \upsilon = 0.75$ whereas the values of parameters β_0 and α are varied in order to explore their effects on the stability of disease free , see Figure (3a). It is obvious that the disease-free equilibrium point (DFE) is locally asymptotically stable for relatively small values of β_0.
In second scenario, we take $\mu = 0.3, d = 0.05, \beta_0 = 0.1, \delta = 0.7, \gamma_1 = 0.4; c_1 = 0.008, c_2 = 0.012, \gamma_2 = 0.5, \sigma_1 = 0.7, \sigma_2 = 0.75, \Omega_1 = 0.8, \Omega_2 = 0.85, \upsilon = 0.75$ whereas the values of parameters β_1 and α are varied in order to investigate their influences on the stability of DFE, see Figure (3b). It is also observed that the DFE is locally asymptotically stable for relatively small values of β_1.
In third scenario, we take $d = 0.05, \beta_0 = 0.1, \beta_1 = 0.15, \delta = 0.7, \gamma_1 = 0.4, c_1 = 0.008, c_2 = 0.012, \gamma_2 = 0.5, \sigma_1 = 0.7, \sigma_2 = 0.75, \Omega_1 = 0.8, \Omega_2 = 0.85, \alpha = 1$ whereas the values of parameters μ and υ are varied, see Figure (3c). It is found that as the vaccination rate increases, the size of stability regions of DFE is enlarged.

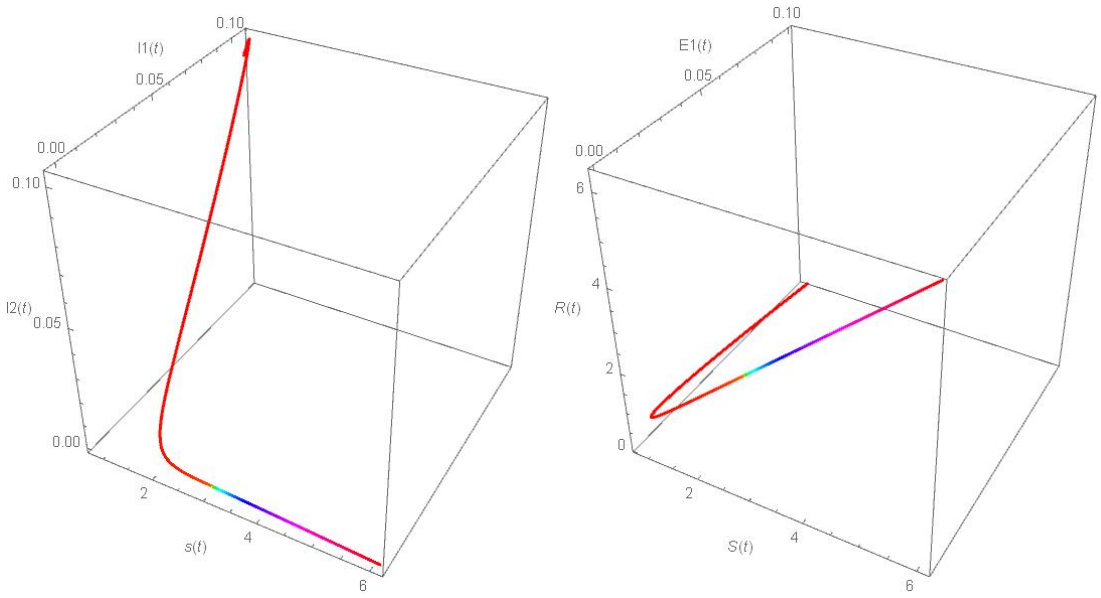

(A) (B)

FIGURE 2. Three dimensional phase portraits of the state variables in system (1) illustrates the local stability of disease free state at $\mu = 0.3, d = 0.05, \delta = 0.7, \gamma_1 = 0.4, \gamma_2 = 0.5, c_1 = 0.008, c_2 = 0.012, \sigma_1 = 0.7, \sigma_2 = 0.75, \Omega_1 = 0.8, \Omega_2 = 0.85, \upsilon = 0.75, \alpha = 1, \beta_0 = 0.15, \beta_1 = 0.1$.

Also, it is shown that as natural birth rate increases, the DFE tends to loss its stability due to the increase in the pool of susceptible individuals.
In fourth scenario, we take $\mu = 0.3, d = 0.05, \beta_0 = 0.1, \beta_1 = 0.18, \delta = 0.7, c_1 = 0.008, c_2 = 0.012, \gamma_1 = 0.4, \gamma_2 = 0.5, \sigma_1 = 0.7, \sigma_2 = 0.75, \Omega_1 = 0.8, \Omega_2 = 0.85$, while the values of parameters υ and α are varied, see Figure(2d). In this case, it is observed that the DFE is stable at relatively large values of vaccination rate.
In fifth scenario, the last values of parameters are used while σ_1 and Ω_1 are changed, see Figure (3e). It is found that the DFE maintains its stability for large values of σ_1 and Ω_1 while DFE losses its stability when one (or both) of these parameters is sufficiently decreased.
Finally, we employ the aforementioned values of parameters with varying υ and γ_1 as shown in Figure (3f). It is observed that the vaccination ratio should be kept above some specific value to render DFE stable and the same is true for recovering rate.

Now, numerical experiments are utilized to examine transcritical bifurcation of the model (1) where the DFE losses its stability and a stable endemic equilibrium point appears in phase space of the system.
First, consider the bifurcation value of $\beta_0 = 0.15$ with the other parameters given by $\mu = 0.3, d = 0.05, \delta = 0.7, \gamma_1 = 0.4, \gamma_2 = 0.5, c_1 = 0.008, c_2 = 0.012, \sigma_1 = 0.7, \sigma_2 = 0.75, \Omega_1 = 0.8, \Omega_2 = 0.85, \alpha = 1, \upsilon = 0.75$ and $\beta_1 = 0.1$

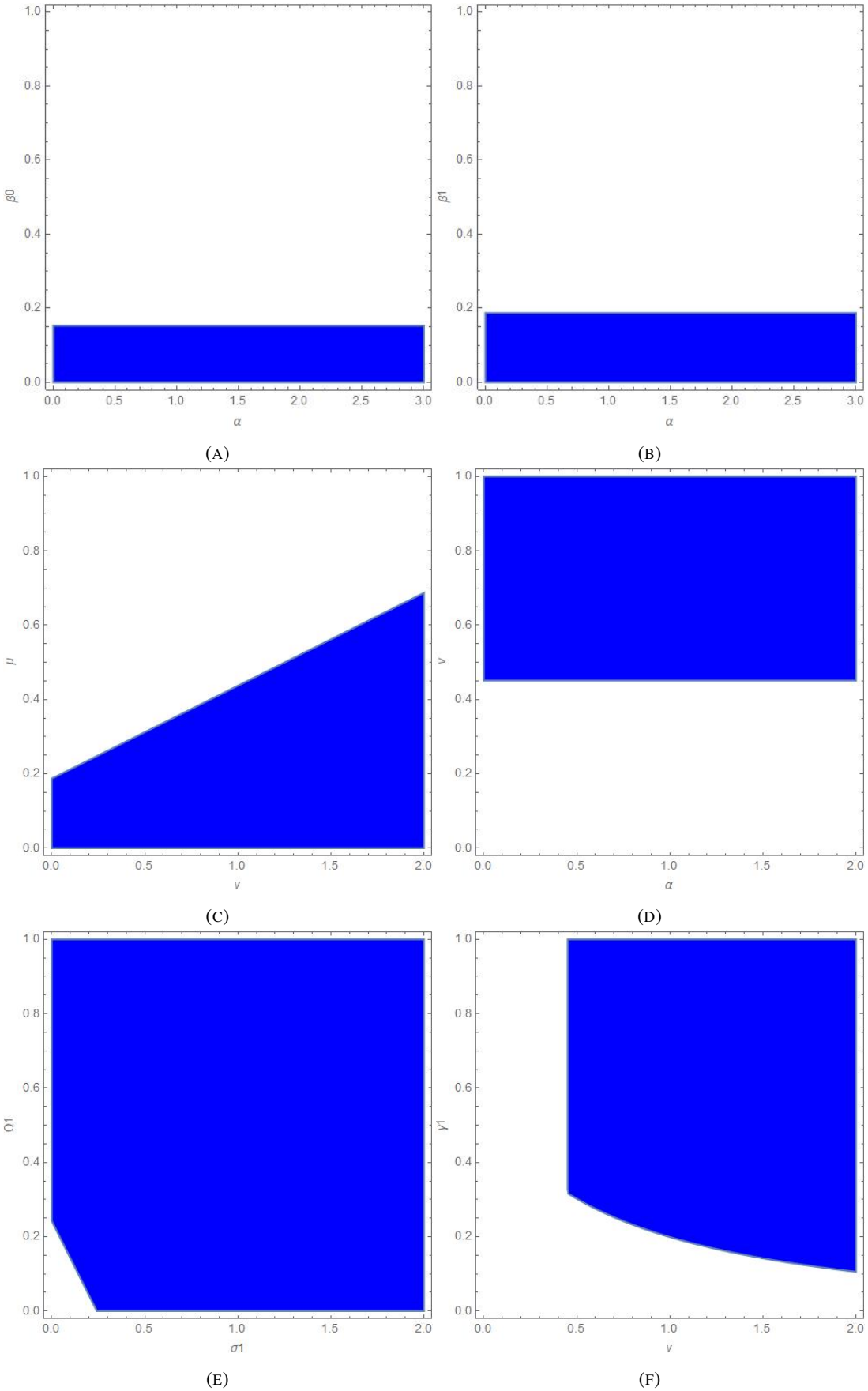

FIGURE 3. Stability region of steady state disease free in different 2D parameters space

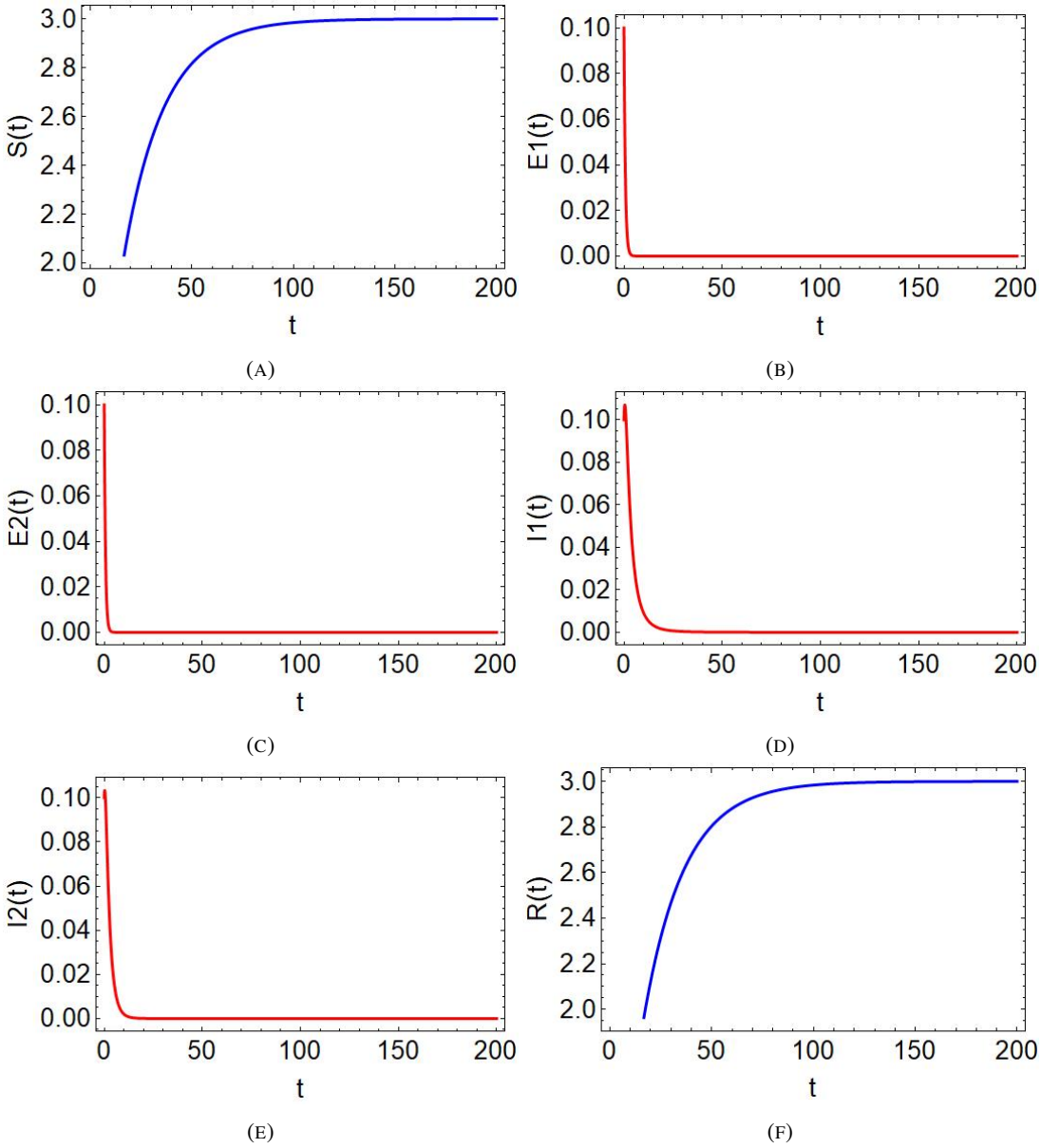

FIGURE 4. Numerical simulations results for $\beta_0 = 0.14$ before transcritical bifurcation point.

The V and W eigenvectors can be expressed as

$$V = \begin{bmatrix} 2.70213 \\ 0 \\ 0 \\ -3.19149 \\ 0 \\ 1 \end{bmatrix},$$

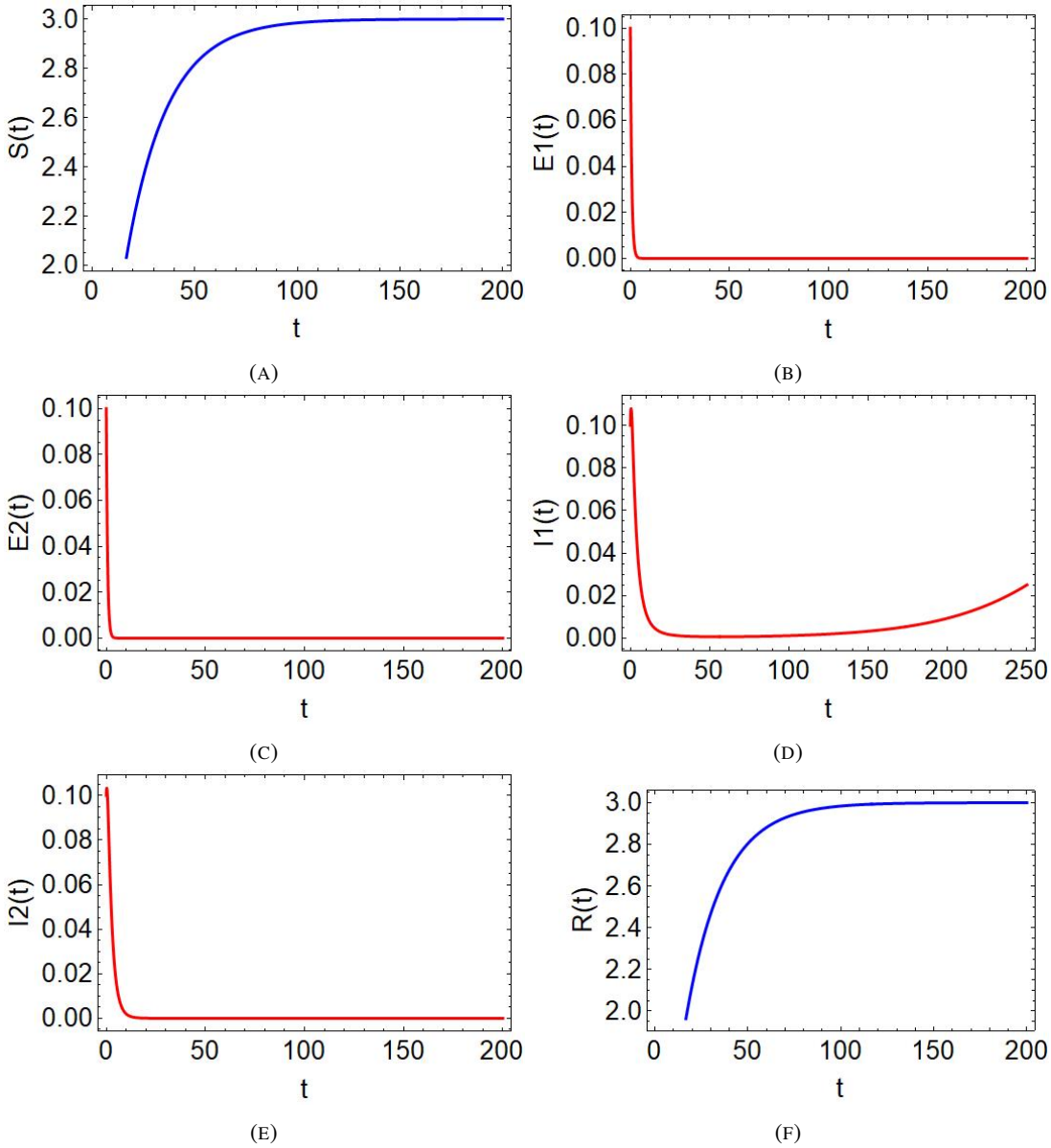

FIGURE 5. Numerical simulations results for $\beta_0 = 0.16$ after transcritical bifurcation point.

$$W = \begin{bmatrix} 0 & 0.636364 & 0 & 1 & 0 & 0 \end{bmatrix},$$

$$V.W = -3.19149$$

.
Then, we get $A = 0$, $B = 0.82505$ and $C = 6$, i.e. the bifurcation is transcritical.
Figure 4 and Figure 5 show the results of numerical simulations of the model (1) before and after occurrence of the bifurcation, respectively. It is obvious that DFE is stable before the bifurcation point. It losses its stability when β_0 passes the bifurcation value and the endemic equilibrium point become stable. More interestingly, it is found that the infected individuals in this case are due to non-mutant virus. The reason is that the value of associated infection rate β_0 is greater than the infection rate β_1 of mutant virus.

In second case, we consider the critical value $\beta_1 = 0.18$ where the other parameters are taken as $\mu = 0.3, d = 0.05, \delta = 0.7, \gamma_1 = 0.4, \gamma_2 = 0.5, c_1 = 0.008, c_2 = 0.012, \sigma_1 = 0.7, \sigma_2 = 0.75, \Omega_1 = 0.8, \Omega_2 = 0.85, \alpha = 1, \upsilon = 0.75$ and $\beta_0 = 0.1$
Similar to previous example, it is obtained that

$$V = \begin{bmatrix} 3.32558 \\ 0 \\ 0 \\ -3.48837 \\ 0 \\ 1 \end{bmatrix},$$

$$W = \begin{bmatrix} 0 & 0.681818 & 0 & 1 & 0 & 0 \end{bmatrix},$$

$$V.W = -3.48837.$$

Thus, it is determined that $A = 0$, $B = 1.24598$ and $C = 6$ in the way that the bifurcation is transcritical. Figure 6 and Figure 7 illustrate the solutions of the model before and after passing the bifurcation value of β_1. It is clear that the DFE is stable before the bifurcation point. Thus, it losses its stability when β_1 passes the bifurcation value and the endemic equilibrium point become stable. More interestingly, it is found that the infected individuals in this case are due to mutant virus only. In other words, the infections of mutant-virus become dominant. The reason is that the value of associated infection rate β_1 is greater than β_0 of the non-mutant virus. This result agrees with available data of health organizations.

Compared with existing results in related works, it is observed that the nonlinear dynamics and control strategies of COVID-19 has been studied in [43] when nonlinear incidence rate is adopted. However, the model in [43] does not involve the influences of vaccination programs and virus mutations, whereas theses effects are considered in our model. A COVID-19 mathematical model incorporating high-risk exposures of Omicron mutant strain has been introduced in [44]. However, the model in [44] employs the simple non-realistic linear incidence rates. In addition, the spatial influences due to movements of individuals from different compartments in their environments are not considered in [44]. A nonlinear controlled SEIR model for COVID-19 pandemic has been presented in [45]. The non-pharmaceutical interventions and vaccination strategies are examined in mathematical model of COVID-19 with comorbidity [46]. The models in [45, 46] use the simple non-realistic linear incidence rates. Moreover, the spatial influences, the exposed individuals who are infectious through the incubation period, and mutant strains of the virus are not considered in [45,46].
A new reaction-diffusion COVID-19 SEIR model with nonlinear incidence rates has been introduced in [47]. The spatio-temporal influences on state variables of the model are included in [47]. Nevertheless, neither the high peril of virus transmission caused by individuals having mild symptoms nor the effects of mutant strains of the virus have been considered in the models [45-47]. The optimal intervention strategies for COVID-19

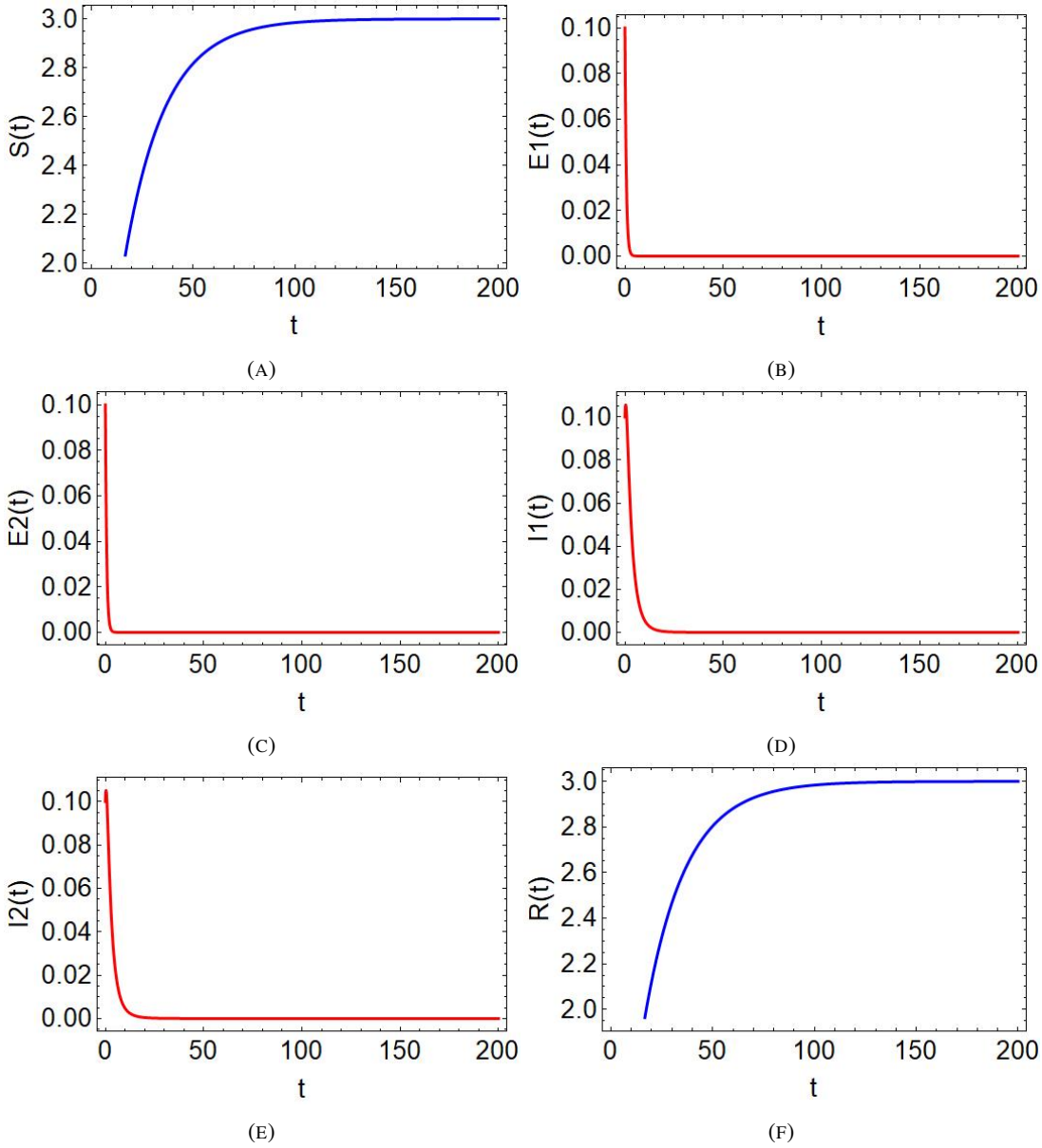

FIGURE 6. Numerical simulations results for $\beta_1 = 0.17$ before occurrence of trans-critical bifurcation

outbreak have been discussed in SAIQJR model [48]. The qualitative behaviors and stability of equilibrium points have been investigated in this model along with basic reproduction number. The aforementioned shortcomings, such as using linear incidence rate and ignoring vaccinations, mutant strains of COVID-19, and combined spatio-temporal dynamics, are still observed in the SAIQJR model.

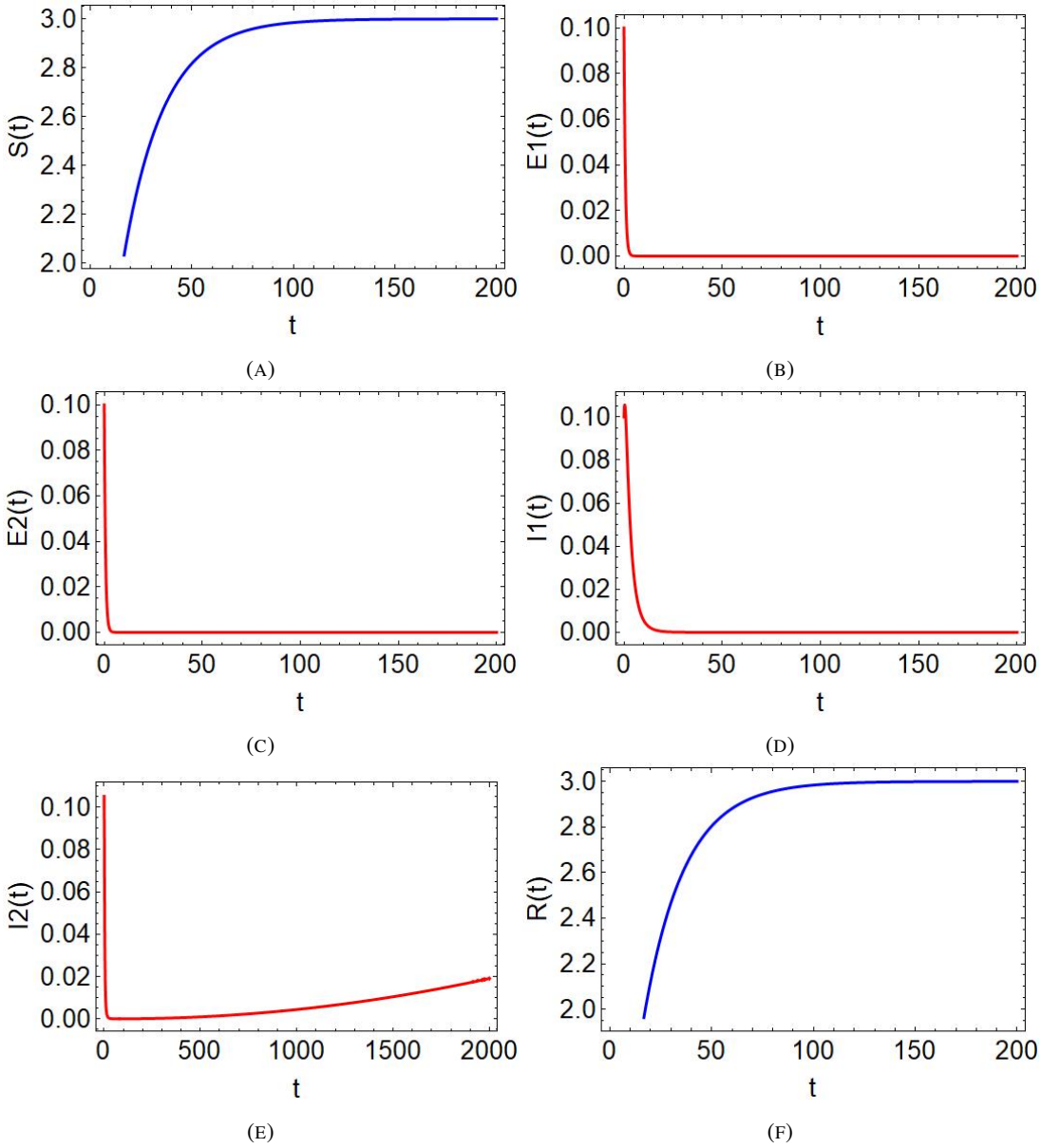

FIGURE 7. Numerical simulations results for $\beta_1 = 0.19$ after occurrence of transcritical bifurcation

The present model in this study addresses all of aforementioned ignored points in recent literature. It is important to note that that eigenvalues of Jacobian matrix can take real values only. This implies that the Hopf bifurcation, Generalized Hopf bifurcation, and Double Hopf bifurcation can not exhibited by the present model as they require pure imaginary eigenvalues at critical bifurcation values.

TABLE 2. Effects of key parameters in the proposed model.

Parameter	Type of variation	Biological meaning
β_0	To increase above β_1	Mutant strain has weak transmission rate
β_1	To increase above β_0	Mutant strain has large transmission rate
γ_2	To increase above γ_1	Treatment methods effectively cure mutant virus infections
δ	Varied from 0 to 1	Incomplete efficiency of vaccines
v	Varied from 0 to 1	Vaccination programs are supported
α	Varied from 0 to 1	Boost interventions and governmental control measures.

TABLE 3. Effects of key parameters in the proposed model (Cont).

Effect	Figure
Most infected individuals are due to non-mutant virus	Fig.8
Most infected individuals are due to mutant virus	Fig.9
Effective suppression of infection cases	Fig.10
Rapid increase of mutant strain infections	Fig.11
Number of mutant virus infections are reduced	Fig.12
Number of mutant virus infections are reduced	Fig.13

Investigating the other possible types of local bifurcations, it is found that the conditions for saddle node and pitchfork bifurcations are not satisfied by our system. The system can undergo transcritical bifurcations as illustrated in bifurcation analysis section.
The observed changes in the dynamics of the proposed model are summarized in the following Table 2 and Table 3 when the key parameters of the model are changed. The bifurcation evolution diagram with varying a bifurcation parameters are presented in Figures 8-13.

7. CONCLUSION

This paper establishes a framework to study the emerging COVID-19 pandemic when virus mutations, vaccination strategies and spatial-temporal variations of populations are considered. The nonlinear incidence rate is employed to include the governmental control actions taken by the governments when the number of infections reaches high levels. The immunity acquired by vaccinations are assumed to be incomplete for realistic considerations. In addition, the proposed model takes in account the realistic scenario that transmission of COVID-19 virus can be caused during incubation period.
Existence, uniqueness and continuous dependence on initial conditions are examined for the solution. Stability analysis and bifurcation analysis are carried out for equilibrium points in the model. It is observed that the vaccination rate should be kept above some specific value to render DFE stable and the same is true for the recovering rate which can be increased by improving health care. More interestingly, in agreement with available data of health organizations, it is found that the infected individuals due to the mutant virus can dominate the infection cases of COVID-19. Theoretical and numerical investigations demonstrate that this can be observed when the infection rate of mutant virus is greater than that of non-mutant virus.
It is known that young individuals are more immune to severe symptoms of COVID-19 compared with elders and those with chronic diseases. However, the present model does not consider this fact in its formulation. So, this crucial point can be considered in future work. It should also be noticed that self-diffusion terms are adopted to simulate the people

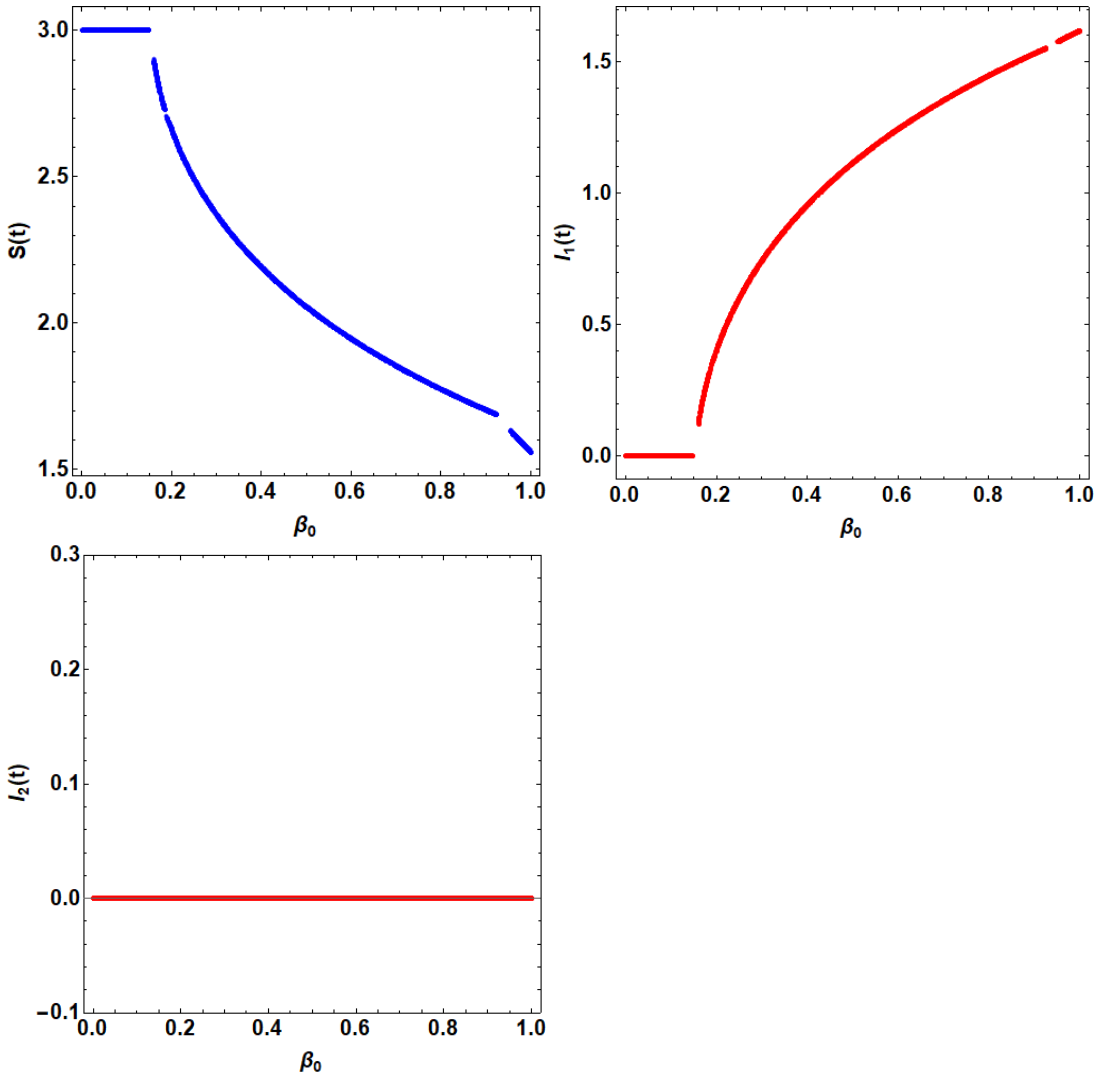

FIGURE 8. The bifurcation diagrams of model state variables vs. β_0. The values of other parameters are $\mu = 0.3, d = 0.05, \delta = 0.7, \gamma_1 = 0.4, \gamma_2 = 0.5, c_1 = 0.008, c_2 = 0.012, \sigma_1 = 0.7, \sigma_2 = 0.75, \Omega_1 = 0.8, \Omega_2 = 0.85, \upsilon = 0.75, \alpha = 1, \beta_1 = 0.1$.

movements in our model. In future work, it would be better to encompass also cross-diffusion dynamics in the model in order to precisely implement the possible types of individuals movements.

REFERENCES

[1] S.H. Strogatz, Nonlinear dynamics and chaos with applications to Physics, Biology, Chemistry, and Engineering, CRC Press, 2018.

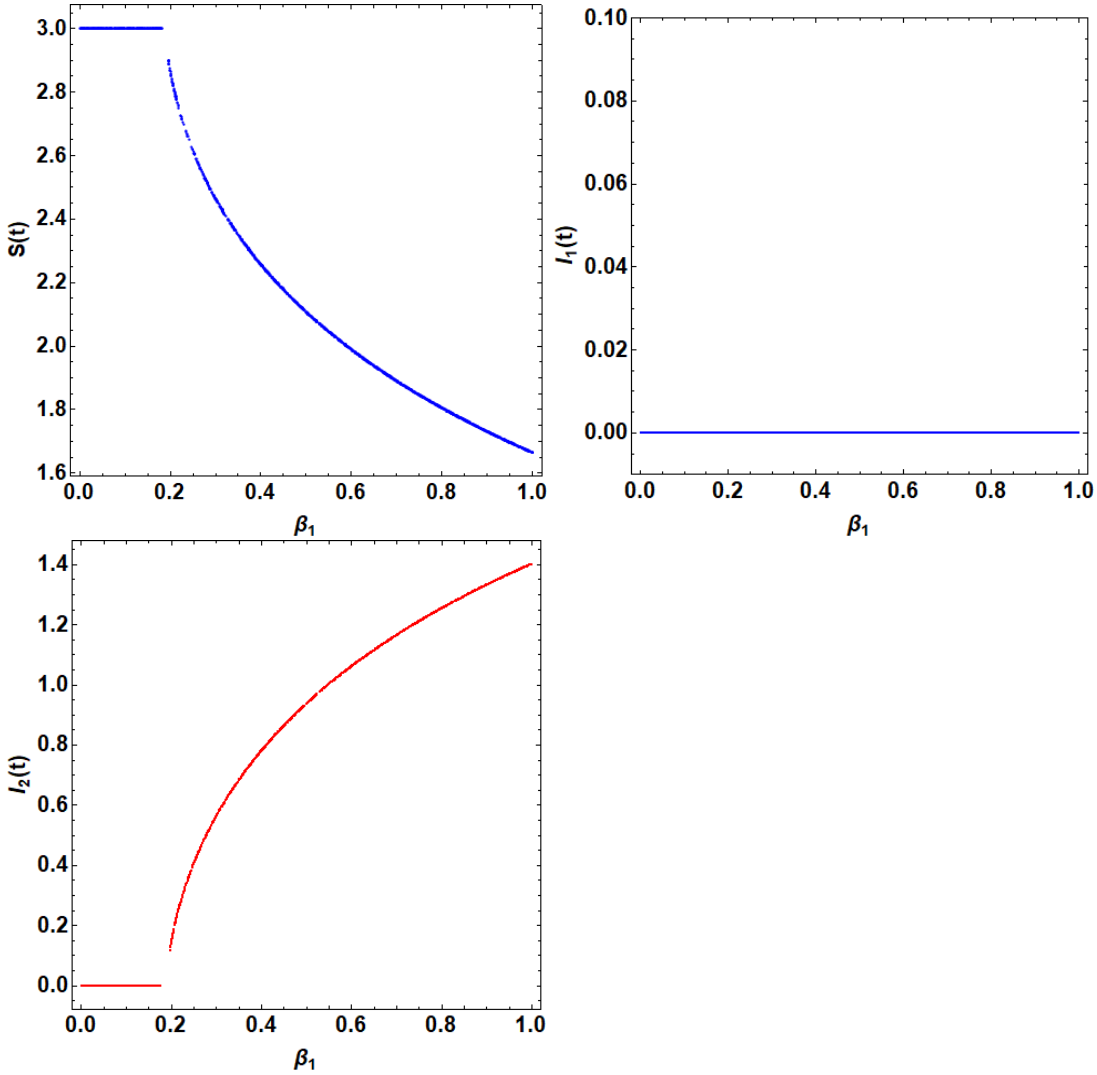

FIGURE 9. The bifurcation diagrams of model state variables vs. β_1. The values of other parameters are $\mu = 0.3, d = 0.05, \delta = 0.7, \gamma_1 = 0.4, \gamma_2 = 0.5, c_1 = 0.008, c_2 = 0.012, \sigma_1 = 0.7, \sigma_2 = 0.75, \Omega_1 = 0.8, \Omega_2 = 0.85, \upsilon = 0.75, \alpha = 1, \beta_0 = 0.1$.

[2] Y. A. Kuznetsov, Elements of applied bifurcation theory, Springer Science & Business Media, 2013.
[3] J. Guckenheimer, P. Holmes, Nonlinear oscillations, dynamical systems, and bifurcations of vector fields, Springer Science & Business Media, 2013.
[4] W.Stephen , S.Wiggins, and M.Golubitsky, Introduction to applied nonlinear dynamical systems and chaos New York(Vol. 2, No. 3), Springer 2003.
[5] Auger, Pierre, de La Parra, R. B., Poggiale, J. C., Sanchez, E., and Sanz, L, Aggregation methods in dynamical systems and applications in population and community dynamics, Physics of Life Reviews, 5(2)2008, 79-105.
[6] E.L.Ionides, C.Breto,and A.Aaron , Inference for nonlinear dynamical systems, Proceedings of the National Academy of Sciences, 103(49) 2006, 18438-18443.

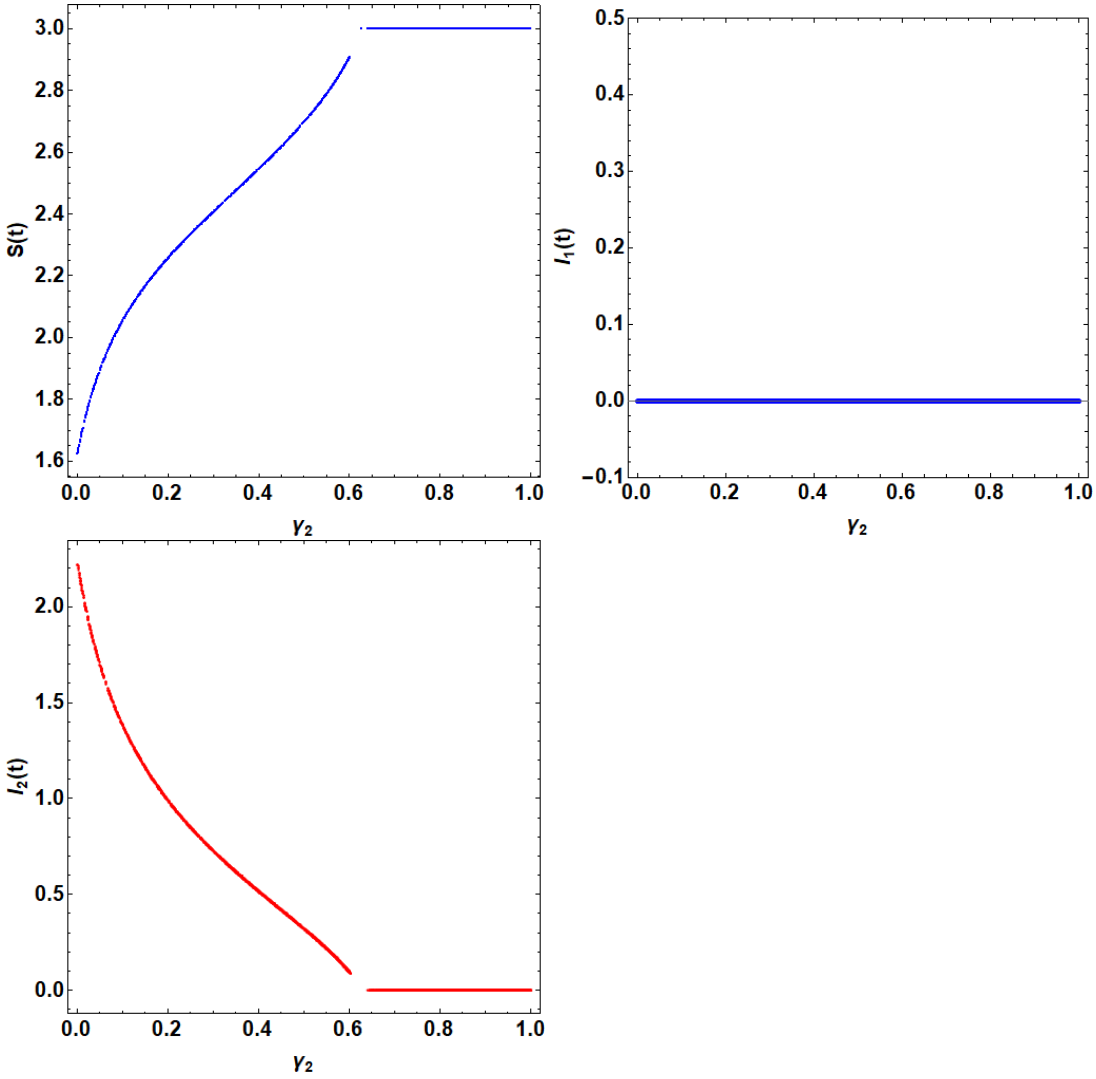

FIGURE 10. The bifurcation diagrams of model state variables vs. γ_2. The values of other parameters are $\mu = 0.3, d = 0.05, \delta = 0.7, \gamma_1 = 0.5, c_1 = 0.008, c_2 = 0.012, \sigma_1 = 0.7, \sigma_2 = 0.75, \Omega_1 = 0.8, \Omega_2 = 0.85, \upsilon = 0.75, \alpha = 1, \beta_0 = 0.1, \beta_1 = 0.23$.

[7] J. M. Meiss, Differential dynamical systems, Society for Industrial and Applied Mathematics 2007.
[8] E. M. Izhikevich, Dynamical Systems in Neuroscience: The Geometry of Excitability and Bursting, Mit Press, 2007.
[9] T.N. Pierre, Dynamical Systems- An Introduction with Applications in Economics and Biology, Springer-Verlag, 1995.
[10] W.Y.Liang, et al. "Design of parallel reservoir computing by mutually-coupled semiconductor lasers with optoelectronic feedback." Optics Communications 495,2021, 127120.

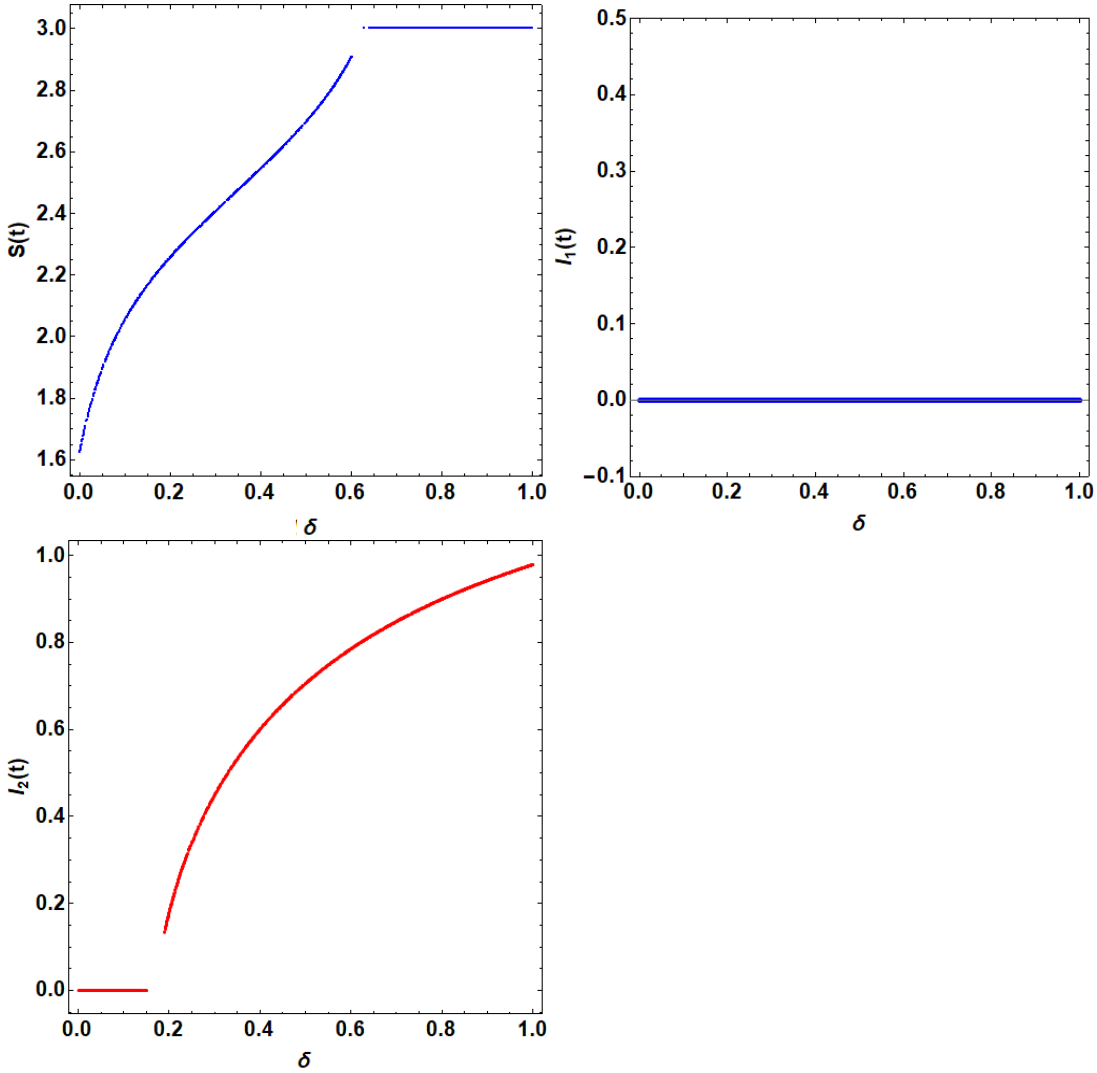

FIGURE 11. The bifurcation diagrams of model state variables vs. δ. The values of other parameters are $\mu = 0.3, d = 0.05, \gamma_1 = 0.5, \gamma_2 = 0.25, c_1 = 0.008, c_2 = 0.012, \sigma_1 = 0.7, \sigma_2 = 0.75, \Omega_1 = 0.8, \Omega_2 = 0.85, \upsilon = 0.75, \alpha = 1, \beta_0 = 0.1, \beta_1 = 0.23$.

[11] X.X. Guo, S.Y. Xiang, Y.H.Zhang, A.J.Wen and Y.Hao, High-speed neuromorphic reservoir computing based on a semiconductor nanolaser with optical feedback under electrical modulation, IEEE Journal of Selected Topics in Quantum Electronics, 26(5)2020, 1-7.

[12] C.Sugano, K. Kanno and A.Uchida, Reservoir computing using multiple lasers with feedback on a photonic integrated circuit, IEEE Journal of Selected Topics in Quantum Electronics, 26(1) 2019, 1-9.

[13] C.I. Siettos, L. Russo, Mathematical modeling of infectious disease dynamics, Virulence, 4(4)2013, 295-306.

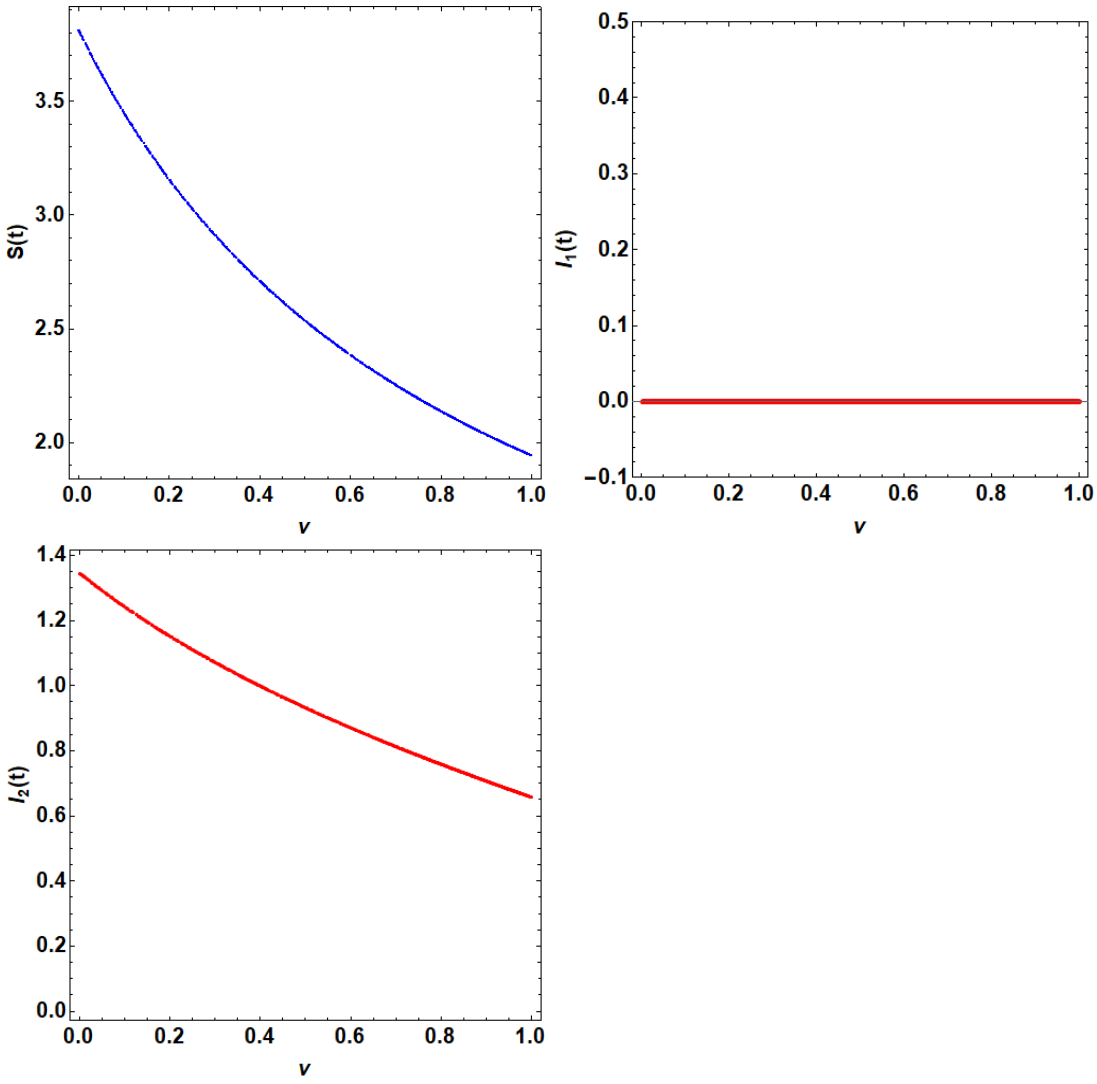

FIGURE 12. The bifurcation diagrams of model state variables vs. v. The values of other parameters are $\mu = 0.3, d = 0.05, \gamma_1 = 0.35, \gamma_2 = 0.25, c_1 = 0.008, c_2 = 0.012, \sigma_1 = 0.7, \sigma_2 = 0.75, \Omega_1 = 0.8, \Omega_2 = 0.85, \delta = 0.6, \alpha = 1, \beta_0 = 0.1, \beta_1 = 0.23$.

[14] S.A. Levin, New directions in the mathematics of infectious disease, In Mathematical approaches for emerging and reemerging infectious diseases: models, methods and theory Springer, New York, NY.2002(pp. 1-5).
[15] V.A. Bokil, Introduction to the mathematics of infectious diseases. Department of Mathematics, Oregon State University, Corvallis, Oregon 2007.
[16] H. Heesterbeek , R.M. Anderson,V. Andreasen et. al, Isaac Newton Institute IDD Collaboration, Modeling infectious disease dynamics in the complex landscape of global health. Science, 347(6227)2015.

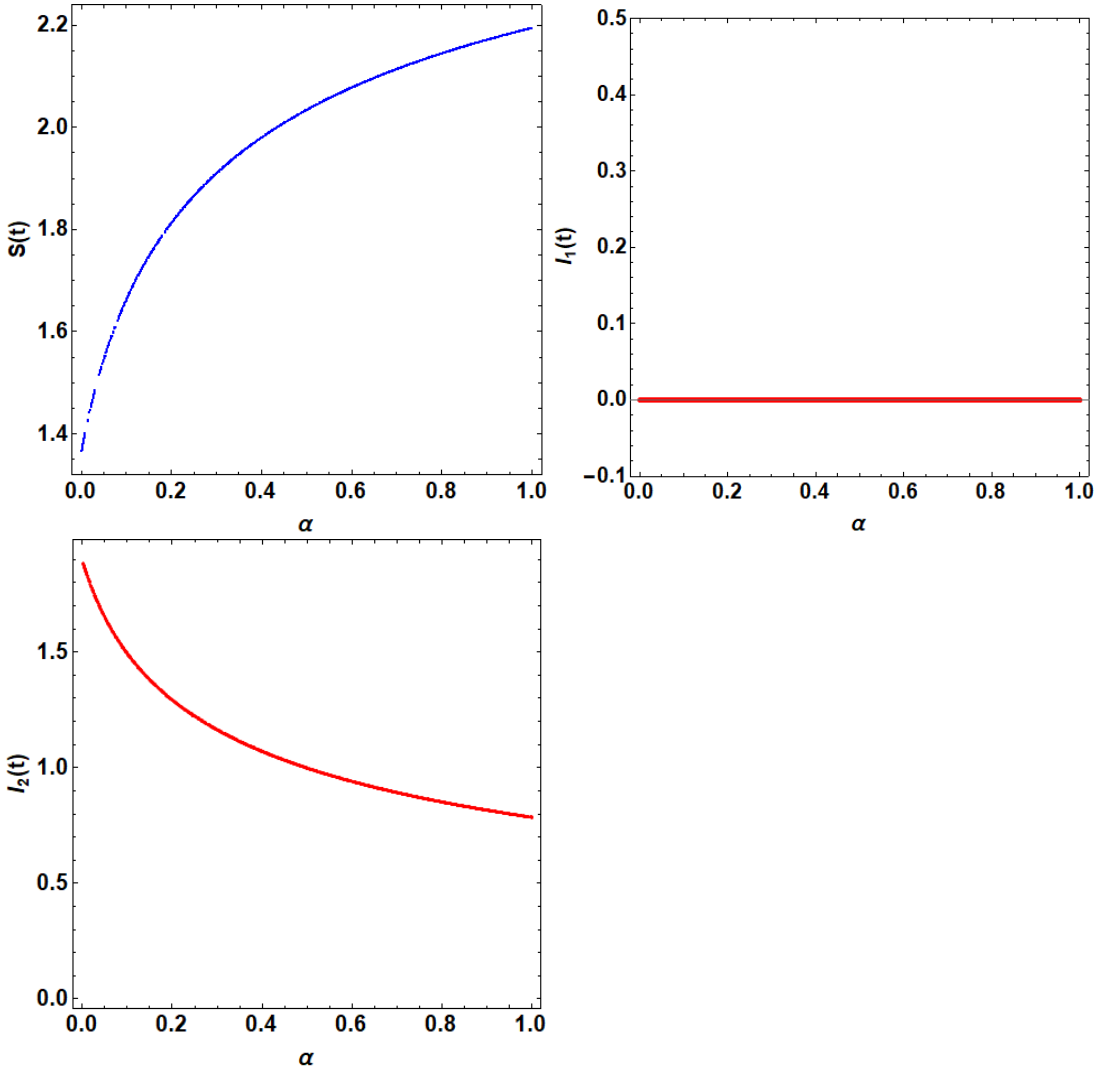

FIGURE 13. The bifurcation diagrams of model state variables vs. α. The values of other parameters are $\mu = 0.3, d = 0.05, \gamma_1 = 0.35, \gamma_2 = 0.25, c_1 = 0.008, c_2 = 0.012, \sigma_1 = 0.7, \sigma_2 = 0.75, \Omega_1 = 0.8, \Omega_2 = 0.85, \upsilon = 0.75, \delta = 0.6, \beta_0 = 0.1, \beta_1 = 0.23$.

[17] M. Bachar, M.A. Khamsi, M. Bounkhel, A mathematical model for the spread of COVID-19 and control mechanisms in Saudi Arabia, Advances in Difference Equations, 2021(1), 1-18.
[18] G. Chowell, L. Sattenspiel, S. Bansal, C. Viboud, Mathematical models to characterize early epidemic growth: A review, Physics of life reviews, 18, 2016, 66-97.
[19] A. Elsonbaty, Z. Sabir, R. Ramaswamy and W.Adel, Dynamical analysis of a novel discrete fractional SITRS model for COVID-19, Fractals, 29(08) 2021, 2140035.

[20] L. Yang, S. Liu, J. Liu, Z. Zhang, X. Wan, B. Huang and Y. Zhang, COVID-19: immunopathogenesis and Immunotherapeutics, Signal transduction and targeted therapy, 5(1)2020, 1-8.
[21] Y.M. Alsofayan, S.M. Althunayyan, A.A. Khan, A.M. Hakawi and A.M. Assiri, Clinical characteristics of COVID-19 in Saudi Arabia: a national retrospective study, Journal of Infection and Public Health, 13(7)2020, 920-925.
[22] E .Elibol, Otolaryngological symptoms in COVID-19, European Archives of Oto-Rhino-Laryngology, 278(4)2021, 1233-1236.
[23] T. Struyf, J. J. Deeks, J. Dinnes, Y. Takwoingi, C. Davenport, M. M. Leeflang, et.al., Signs and symptoms to determine if a patient presenting in primary care or hospital outpatient settings has COVID-19, Cochrane Database of Systematic Reviews, (5)2022.
[24] R.M. El-Shabasy, M.A. Nayel, M.M Taher, R. Abdelmonem, and K.R. Shoueir, Three wave changes, new variant strains, and vaccination effect against COVID-19 pandemic, International Journal of Biological Macromolecules 2022.
[25] A. Kronbichler, D. Kresse, S. Yoon, K. H. Lee, M. Effenberger, and J.I. Shin, Asymptomatic patients as a source of COVID-19 infections: A systematic review and meta-analysis, International journal of infectious diseases 98 2020, 180-186.
[26] L. Cao and Q. Liu, COVID-19 modeling: A review, medRxiv 2022.
[27] Y. Demirbilek, G. Pehlivanturk, Z.O. Ozguler,E.A. Mese, COVID-19 outbreak control, example of ministry of health of Turkey. Turkish journal of medical sciences, 50(9)2020, 489-494.
[28] S.M. Alghamdi, J.S. Alqahtani, A.M. Aldhahir, Current status of telehealth in Saudi Arabia during COVID-19. Journal of family and community medicine, 27(3)2020, 208.
[29] G. Stewart, K. Heusden,G.A. Dumont, How control theory can help us control COVID-19, IEEE Spectrum, 57(6)2020, 22-29.
[30] B. Robson, COVID-19 Coronavirus spike protein analysis for synthetic vaccines, a peptidomimetic antagonist and therapeutic drugs, and analysis of a proposed achilles heel conserved region to minimize probability of escape mutations and drug resistance. Computers in biology and medicine, 121,2020, 103749.
[31] D. Duong ,Alpha,Beta,Delta,Gamma:What is important to know about SARS-CoV-2 variants of concerc ,2021,E1059-E1060.
[32] Y. Araf, F. Akter, Y.D. Tang, R. Fatemi, M.S.A. Parvez, C. Zheng and M.G. Hossain, Omicron variant of SARS-CoV-2: genomics, transmissibility, and responses to current COVID-19 vaccines, Journal of medical virology, 94(5)2022, 1825-1832.
[33] E. Takashita, N. Kinoshita, S. Yamayoshi, Efficacy of antibodies and antiviral drugs against Covid-19 omicron variant, New England Journal of Medicine, 386(10)2022, 995-998.
[34] R.M. Jena, S. Chakraverty, D. Baleanu, SIR epidemic model of childhood diseases through fractional operators with Mittag-Leffler and exponential kernels. Mathematics and Computers in Simulation, 182, 2021, 514-534.
[35] M. Parsamanesh, M. Erfanian, Global dynamics of an epidemic model with standard incidence rate and vaccination strategy. Chaos, Solitons & Fractals, 117, 2018, 192-199.
[36] M. Parsamanesh, M. Erfanian, Stability and bifurcations in a discrete-time SIVS model with saturated incidence rate. Chaos, Solitons & Fractals, 150, 2021, 111178.
[37] B. Li, H. Liang, Q. He, Multiple and generic bifurcation analysis of a discrete Hindmarsh-Rose model. Chaos, Solitons & Fractals, 146, 2021, 110856.
[38] H.M. Ali, I.G. Ameen, Optimal control strategies of a fractional order model for zika virus infection involving various transmissions. Chaos, Solitons & Fractals, 146, 2021, 110864.
[39] M. Parsamanesh, M. Erfanian, S. Mehrshad, Stability and bifurcations in a discrete-time epidemic model with vaccination and vital dynamics. BMC bioinformatics, 21(1), 2020, 1-15.
[40] O. Diekmann, J. Heesterbeek, M.G. Roberts, The construction of next-generation matrices for compartmental epidemic models, J R Soc Interface 7(47)2010, 873–885.
[41] P. van den Driessche, J. Watmough, Further notes on the basic reproduction number, in Mathematical Epidemiology, Springer, Berlin, Heidelberg,2008, pp 159–17.
[42] P. Samui, J. Mondal, S. Khajanchi, A mathematical model for COVID-19 transmission dynamics with a case study of India, Chaos Solit Fract 140, 2020 ,110173
[43] G. Rohith, K. B. Devika, Dynamics and control of COVID-19 pandemic with nonlinear incidence rates. Nonlinear Dynamics, 101(3), 2020, 2013-2026.
[44] T. Li, Y. Guo, Optimal control and cost-effectiveness analysis of a new COVID-19 model for Omicron strain. Physica A: Statistical Mechanics and its Applications, 606, 2022, 128134.
[45] V. Piccirillo, Nonlinear control of infection spread based on a deterministic SEIR model. Chaos, Solitons & Fractals, 149, 2021, 111051.
[46] P. Das, R. K. Upadhyay, A. K. Misra, F. A. Rihan, P. Das, D. Ghosh, Mathematical model of COVID-19 with comorbidity and controlling using non-pharmaceutical interventions and vaccination. Nonlinear Dynamics, 106(2), 2021, 1213-1227.
[47] N. Ahmed, A. Elsonbaty, A. Raza, M. Rafiq, W. Adel, Numerical simulation and stability analysis of a novel reaction-diffusion COVID-19 model. Nonlinear Dynamics, 106(2), 2021, 1293-1310.
[48] J. Mondal, S. Khajanchi, Mathematical modeling and optimal intervention strategies of the COVID-19 outbreak. Nonlinear dynamics, 109, 2022, 177-202.

[1] Department of Mathematics,College of Science and Humanities in Al-Kharj, Prince Sattam bin Abdulaziz University, Al-Kharj 11942, Saudi Arabia.
Email address: s.h.m33@hotmail.com

[2] Department of Basic Science, Faculty of Computers and Informatics, Suez Canal University, Ismailia, Egypt.
Email address: aelsadany1@yahoo.com

[3] Mathematics and Engineering Physics Department, Faculty of Engineering, Mansoura University, PO 35516, Mansoura, Egypt.
Email address: sonbaty2010@gmail.com